Sci

MDPI

Article

AI, Grain Use Efficiency, and Food Security in China: A Quantitative Assessment Using the Supply–Demand Relaxation Effect (SRE)

Akira Toyohara *,† and Weisheng Zhou *

Graduate School of Policy Science, Ritsumeikan University, 2-150 Iwakura-cho, Ibaraki 567-8570, Osaka, Japan
* Correspondence: ps0601sh@ed.ritsumei.ac.jp (A.T.); zhou@sps.ritsumei.ac.jp (W.Z.)
† Graduate student researcher.

Abstract

Artificial intelligence (AI) adoption in agriculture does more than replace labor: it reorganizes how efficiently grain is used and stored. We formalize AI's relaxation capacity as the dimensionless Supply–Demand Relaxation Effect (SRE), decompose it into five pathways (labor displacement, improvement in the feed conversion ratio (FCR), industrial AI, precision agriculture, and loss reduction), and evaluate it across the 27 empirically anchored scenarios of our published baseline study. The largest demand-side effect is FCR improvement, one to two orders of magnitude larger than labor displacement. With population declining, self-sufficiency arrives regardless of AI (2039–2079 in the baseline); AI advances it by 2–11 years. The effect grows with scenario severity: 3–5 years under optimistic scenarios but 6–11 years under the worst, and the 2100 surplus gain rises from 5–10% to 26–47%. AI's marginal value is greatest where the food balance is tightest, so the higher the population target, the closer AI investment comes to a necessary condition. Precision agriculture has the larger effect, but FCR improvement (precision livestock AI) should rank highest, because it is supply-scenario-independent and unlikely to be delivered by the market. Realizing the precision-agriculture gain requires public investment in rural digital infrastructure to bridge China's regional divide.

Keywords: grain use efficiency; feed conversion ratio (FCR); precision livestock AI; supply–demand relaxation effect (SRE); China food security

1. Introduction

China accounts for approximately 17% of the world's population [1] while facing structural vulnerabilities in food security [2]. Maintaining arable land at or above the minimum conservation line that the government sets as a food-security floor (the "red line", 120 million ha = 1.8 billion mu) is a persistent challenge [2], and import dependence, driven primarily by soybeans, currently stands at around 15% (the 2024 gap of 124 Mt against a demand of 831 Mt, computed from the same source). Population decline toward 2100 (460 million under this study's medium scenario, P2) will ease long-term demand pressure, but large-scale import dependence is still projected for the 2020s–2050s [2]. Meanwhile, domestic production expanded from 462 Mt in 2000 [2] to 706.5 Mt in 2024 (total grain output) [3], and in the 2020s China entered a phase of full-scale deployment of digital and artificial intelligence (AI) technologies in agriculture. In 2023, the annual cumulative operating area of China's plant-protection drones reached 2.13 billion mu-times (about

Check for updates

Received: 15 July 2026
Revised: 17 August 2026
Accepted: 20 August 2026
Published: 26 August 2026

Copyright: © 2026 by the authors. Licensee MDPI, Basel, Switzerland. This article is an open access article distributed under the terms and conditions of the Creative Commons Attribution (CC BY) license.

142 million ha) [4]—a cumulative value that double-counts repeat applications on the same field, so the actual cropland covered is only a fraction of this figure, and no official statistic for the unique coverage rate is published. Yet studies assessing the effects of these AI technologies on food supply and demand remain scarce.

AI and robotic technologies are diffusing rapidly across both agriculture and the food industry. Smart farming (precision agriculture, drone-based monitoring, and sensing based on the Internet of Things, or IoT) improves yields and resource efficiency [5], and the proposition that "AI produces but does not consume" creates an intuitive expectation that AI adoption only strengthens the supply side. In practice, however, AI also reshapes how efficiently grain is used as feed and industrial feedstock, and how much of it is lost in storage. Because AI adoption simultaneously induces supply augmentation and demand rationalization, its policy implications cannot be derived without an integrated assessment of both.

Existing reviews of AI in agriculture have focused on the accuracy of recognition and prediction tasks at the production site (disease detection, crop classification, and yield prediction) [6] or on the technological base of data use and the governance and business models along the supply chain [7]. Neither strand systematically examines the spillover to the demand side. In precision livestock science, real-time sensing for animal health and productivity [8] and improvements in feed efficiency through precision feeding [9] have been reported, and in animal breeding the acceleration of genetic gain through genomic selection has been noted [10]; however, few studies connect these to a food supply–demand model. On the long-run food supply–demand side, work has accumulated, including estimates of world demand in 2050 [11] and a 27-scenario analysis of China's food balance sheet based on data from the National Bureau of Statistics of China (NBS) [2]; neither takes AI effects into account. The gap in prior research lies in quantitatively incorporating demand-rationalization effects, including improvement in the feed conversion ratio (FCR) and loss reduction through precision livestock and precision agriculture, into a long-term food supply–demand model, and this study fills that gap.

China's food supply and demand can be organized into a three-layer structure: a human consumption layer (layer 1) comprising population and per-capita consumption, a biological conversion layer (layer 2) mediated by meat consumption and feed conversion, and a governance layer (layer 3) in which AI participates in production while not itself consuming. We focus on the third of these (the AI governance layer) and superimpose the additional effects of AI on the 27 scenarios of Toyohara and Zhou [2], which serve as the baseline. That baseline study quantified China's long-run food balance in the absence of AI; the present paper is its AI extension, and everything reported here—the indicator, the pathway decomposition, and the timing analysis—is new relative to it. Our contribution is threefold. We first formalize the bidirectional effects of the adoption of AI and robotics on food supply and demand as the Supply–Demand Relaxation Effect (SRE), a dimensionless indicator that is contrasted systematically with the conventional food-security metrics (the self-sufficiency ratio, the import dependency ratio, and the supply–demand gap) in Table 1 of Section 2.1. We then decompose SRE into five pathways (labor displacement, FCR improvement, industrial AI, precision agriculture, and loss reduction) and estimate the magnitude of each. We then evaluate the additional yield improvement from AI precision agriculture ($\rho_{\mathrm{PA}} = 2$–6%) and present an S-O+ scenario ($S^{+}_{2100} = 1248$ Mt) that exceeds the baseline supply trajectory.

Table 1. Positioning of SRE relative to existing food-security indicators.

Indicator	Category	Description
Food Security Index	Outcome (composite score)	E.g., the Global Food Security Index (GFSI). A ranking index combining availability, affordability, and quality; the contribution of an individual technology cannot be isolated
Self-sufficiency Ratio	Outcome	Domestic production/total demand. A static ratio indicating the outcome of supply and demand
Import Dependency	Outcome	Imports/total demand. A static ratio indicating the outcome of external dependence
Supply Gap (G_t)	State	Demand—supply. The level of supply–demand imbalance at a given point in time
SRE (this study)	Capacity for AI-driven improvement	A dimensionless flow indicator measuring how much an intervention (AI adoption) can relax the supply–demand gap. It quantifies the "marginal contribution of a technology" that existing indicators cannot measure

Note: The self-sufficiency ratio, import dependency, and supply gap describe the state or outcome of supply and demand, but cannot isolate the improvement contribution of a specific technology. The SRE fills this gap, quantifying the effect of interventions such as AI in a form amenable to policy comparison.

2. Analytical Framework

2.1. Basic Formulation

This section defines the supply–demand gap and the Supply–Demand Relaxation Effect (SRE) used to assess AI effects, and specifies the baseline scenario system and analysis period. First, the food supply–demand gap G_t at time t is defined as

$$G_t = D_t - S_t \tag{1}$$

where $D_t = P_t \times C_t^*$ is total demand (P_t: population; C_t^*: per-capita grain-equivalent consumption in kg/year), and S_t is domestic production (Mt). $G_t > 0$ denotes import dependence (deficit) in which demand exceeds domestic production; $G_t = 0$ denotes self-sufficiency, a state in which supply and demand are balanced; and $G_t < 0$ denotes a food surplus in which domestic production exceeds demand. Because C^* is an aggregate grain-equivalent indicator, a surplus is to be read throughout in grain-equivalent terms: $G_t < 0$ indicates surplus capacity in the aggregate balance, not realized export capacity, or food security in the full sense, since it abstracts from trade arrangements, reserve policy, and commodity composition (soybeans in particular; see the limitations in Section 4.3). This delimitation can be stated more generally. Food security is a multidimensional concept that the FAO framework divides into four dimensions: availability, access, utilization, and stability [12]. The SRE framework of this study addresses the aggregate availability dimension alone; affordability and distributional access, nutritional quality, and the stability of access under shocks lie outside its scope. Self-sufficiency and surplus in this paper are therefore to be read as statements about the aggregate physical balance, not as a full assessment of food security.

AI adoption pushes this gap down by raising supply and lowering demand. We define the post-AI gap as

$$G_t^{\mathrm{AI}} = G_{\mathrm{baseline},t} - \left(\Delta S_t^{\mathrm{AI}} + \Delta D_t^{\mathrm{AI}}\right) \tag{2}$$

where $\Delta S_t^{\mathrm{AI}} > 0$ is the AI-induced increase in supply, $\Delta D_t^{\mathrm{AI}} > 0$ the AI-induced reduction in demand (both defined as positive), and $G_{\mathrm{baseline},t}$ the baseline gap without AI. Self-

sufficiency is attained when $G_t^{\mathrm{AI}} \leq 0$, which holds if either the baseline is already in surplus ($G_{\mathrm{baseline},t} \leq 0$) or the AI effect exceeds the gap.

One point warrants care. Because China's population declines throughout this century, the baseline gap $G_{\mathrm{baseline},t}$ turns from positive to negative with or without AI, and self-sufficiency is eventually attained (Section 3.5). A ratio with the time-varying $G_{\mathrm{baseline},t}$ in its denominator would therefore diverge near the year of self-sufficiency, where the denominator approaches zero. We accordingly normalize the relaxation capacity of AI against a fixed reference gap:

$$\mathrm{SRE}_t = \frac{\Delta S_t^{\mathrm{AI}} + \Delta D_t^{\mathrm{AI}}}{|G_{\mathrm{ref}}|}, \qquad G_{\mathrm{ref}} = G_{\mathrm{baseline},2030} = 112.26\ \mathrm{Mt} \tag{3}$$

G_{ref} is the baseline gap in 2030 and is taken to represent the transitional period during which China's dependence on food imports is heaviest. The value is stated to two decimal places here, and used at that precision throughout, so that the pathway decomposition in Section 3.4 reproduces exactly. The baseline here is the reference case of the 27-scenario system introduced below, namely the combination of the medium population P2, the medium demand D-M, and the optimistic supply S-O (P2 × D-M × S-O) (#13 of Toyohara and Zhou [2]). From that table, $D_{2030} = 1387$ million $\times$ 626 kg/person/year $= 868.26$ Mt and $S_{2030} = 756$ Mt, so that $G_{\mathrm{ref}} = 112.26$ Mt; for readability this value is rounded to 112 Mt in the text, while all SRE values are computed from the precise 112.26 Mt. Because we recompute the product from the published rounded entries, this differs slightly from the 111 Mt (12.8%) reported for the same year by Toyohara and Zhou [2] from unrounded internals; the difference is one of rounding alone. The SRE is thus a dimensionless measure of magnitude, namely how much AI can shift the balance relative to the gap of the transitional period, and says nothing about whether the future gap is closed. SRE = 1 means only that the relaxation capacity of AI is of the same magnitude as the reference gap.

What the AI effect delivers depends on the period. Before self-sufficiency it shrinks the gap, lowering import dependence and bringing forward the year of self-sufficiency. After self-sufficiency the same magnitude appears as a thickening of the grain-equivalent surplus, strengthening strategic reserves and resilience to climate shocks. The numerator $\Delta S_t^{\mathrm{AI}} + \Delta D_t^{\mathrm{AI}}$ is meaningful in both periods.

The novelty of the SRE is that, whereas existing food-security indicators measure a "state" or an "outcome", it measures the "capacity for improvement (a flow)" generated by a specific intervention (AI adoption). The self-sufficiency ratio and the import dependency ratio describe the outcome of supply and demand, and the supply gap G_t describes the state of supply and demand; these are static indicators, and none of them can assess how much a given technology can shift that state. By placing the intervention effect ($\Delta S^{\mathrm{AI}} + \Delta D^{\mathrm{AI}}$) in the numerator and the transitional-period reference gap $|G_{\mathrm{ref}}|$ in the denominator, the SRE quantifies the marginal improvement capacity of an intervention as a dimensionless quantity (Table 1). This allows the relaxation effects of different AI technologies and deployment scenarios to be compared on a common scale, and can be used directly to prioritize policy investment.

The effects of AI technology are not maximized upon adoption but emerge gradually as the technology diffuses. The AI adoption rate $A(t) \in [0, 1]$ is represented by a logistic function:

$$A(t) = \frac{1}{1 + \exp\big(-k(t - t_0)\big)} \tag{4}$$

where k denotes the diffusion speed and t_0 the inflection year. Neither parameter can be calibrated from data: no nationwide time series exists for the adoption of agricultural AI in China, and the frequently cited statistics on the operating area of agricultural drones measure cumulative work volume rather than an adoption rate. We therefore treat k and t_0

not as estimates but as diffusion scenarios. Rather than assuming the abstract parameters k and t_0 directly, we assume an interpretable quantity, namely how much of the chosen deployment scenario is realized by a given year, and back out k and t_0 from it (Table 2).

Table 2. AI diffusion scenarios (defined by realization rates; k and t_0 are back-solved).

Diffusion Scenario	$A(2030)$	$A(2050)$	k	t_0
Early	55%	90%	0.100	2028
Central (reference)	**40%**	**73%**	**0.070**	**2036**
Late	25%	55%	0.065	2047

Note: Bold marks the reference (central) diffusion scenario. $A(t)$ is the realization rate of the chosen deployment scenario, not the share of farms that have adopted AI. We assume $A(2030)$ and $A(2050)$ and back-solve k and t_0 from Equation (4). All three scenarios reach $A(2100) \geq 0.97$ (early 1.00, central 0.99, late 0.97), so the maturity value SRE_∞ does not depend on the diffusion scenario.

Central diffusion is a conservative reference, reflecting the fact that agricultural technology depends on capital investment in machinery, sensors, and rural communication infrastructure, and so diffuses more slowly than consumer goods. Its inflection year $t_0 = 2036$ is the midpoint of the transition of agricultural AI and precision livestock farming from the pilot-introduction phase (mid-2010s) to full-scale deployment, and corresponds to the timing of China's digital agriculture policies such as the "Digital Village" plan. Two observable anchors support placing the midpoint in the mid-2030s rather than earlier or later. First, China's rural-digitalization policy sets its own long-range milestones at 2035: the Digital Village Development Strategy Outline schedules "substantial progress" for that year [13], so the midpoint back-solved from the realization-rate assumptions of Table 2 ($t_0 = 2035.8$, rounded to 2036) falls almost exactly on the official milestone, tracking the policy timetable rather than assuming acceleration beyond it. Second, the observed diffusion of the most visible technology, plant-protection drones, is consistent with the early segment of the central curve: operations reached 2.13–2.67 billion mu-times in 2023–2024 [4,14], and are still growing at roughly 25–37% per year (25% from the 2023–2024 increase and 36.5% from the year-on-year rate reported for 2023; a doubling time of two to three years), far from saturation; this is consistent with the central scenario, in which the midpoint of realization ($t_0 = 2036$) still lies more than a decade ahead. Because neither anchor pins the parameter tightly, the early ($t_0 = 2028$) and late ($t_0 = 2047$) scenarios, nearly two decades apart, carry the remaining uncertainty. Early diffusion corresponds to rapid market-led uptake, late diffusion to stalled penetration among small-scale farms.

All three diffusion scenarios reach $A(2100) \geq 0.97$ and thus produce virtually no difference in the effect magnitude at maturity. What the diffusion scenario governs is the timing at which the relaxation is attained, not the level attained, that is, SRE_∞ (Section 3.6). The central question of this study—how much AI can relax the supply–demand balance—can consequently be answered independently of the diffusion speed, which cannot be calibrated. Uncertainty about the ceiling of the effect itself is carried by the three deployment scenarios (moderate, aggressive, full), and $A(t) \to 1$ means not that every farm adopts AI but that the chosen deployment scenario is fully realized. The effects on supply and demand are assumed to emerge in proportion to the adoption rate, and are therefore expressed in terms of their magnitudes at maturity (subscript ∞, i.e., when the technology is fully diffused) as

$$\Delta S_t^{\mathrm{AI}} = \Delta S_\infty^{\mathrm{AI}} A(t), \qquad \Delta D_t^{\mathrm{AI}} = \Delta D_\infty^{\mathrm{AI}} A(t) \tag{5}$$

This gives $\mathrm{SRE}_t = \mathrm{SRE}_\infty A(t)$, so the SRE converges to its maturity upper bound as diffusion progresses. Under the central diffusion scenario, $A(2030) \approx 0.40$ and $A(2100) \approx 0.99$; this study treats 2100 as maturity ($A \approx 1$). Applying a common $A(t)$ to all five pathways is a

deliberate simplification; the bias it introduces is quantified by a bounding check in Section 3.6 (the maturity value is exactly invariant, the transient deviation is at most 0.06 in 2030 and 0.17 at mid-century, and the common curve errs on the conservative side).

The analysis uses the 27-scenario system of Toyohara and Zhou [2] as its baseline. The system combines three levels on each of three axes (population, demand, supply), yielding 27 cases (Table 3).

Table 3. Baseline scenario system and trajectories of the main variables [2].

Scenario	2020	2030	2050	2080	2100
Population P_t (million)					
P1 (low)	1412	1373	1110	530	320
P2 (medium)	1412	1387	1194	734	460
P3 (policy target)	1412	1403	1290	945	700
Demand D (C_t^*: kg/person/year)					
D-L (East Asian saturation)	583	615	680	662	650
D-M (EU type)	583	626	740	764	780
D-H (EU+α type)	583	640	800	830	850
Supply S_t (Mt)					
S-O (optimistic)	669	756	918	1087	1200
S-M (medium)	669	720	850	958	1030
S-P (pessimistic)	669	680	760	820	860

Source: Toyohara and Zhou [2]. Population figures are the decadal estimates of that study (P1/P2/P3 correspond to its S1/S2/S5, with constant total fertility rates (TFRs) of 0.75, 1.00, and 1.31, respectively). The 2030/2050/2100 values for demand and supply follow the same source; 2020 is observed and 2080 is a linear interpolation between 2050 and 2100. The 2080 column is therefore illustrative only: the trajectory used in Sections 3.5 and 3.6 additionally carries the 2075 keypoint of the source, and consequently departs from this column between 2050 and 2100.

The content of each level follows Toyohara and Zhou [2] and may be summarized as follows. On the population axis, P1 (low; 320 million in 2100) is a trajectory in which the total fertility rate falls to the Korean level of 0.75 and remains fixed there, while P2 (medium; 460 million) is a status-quo trajectory in which the official statistical value of 1.01 (held at approximately 1.0 in the scenario) simply persists. P3 (policy target; 700 million) is not an independent demographic projection but a reference scenario for policy debate, anchored on halving the 2021 population peak of 1412 million; the fertility rate of approximately 1.31 required to reach 700 million by 2100 is obtained by back-calculation. The demand axis is defined by the terminal level of per-capita grain-equivalent consumption C_{2100}^*: D-L (650 kg/person/year) corresponds to the East Asian saturation level exhibited by Japan and Korea, D-M (780) to a gradual EU-type upward trajectory, and D-H (850) to a high saturation case lying between the EU average (700) and the United States (1100). The supply axis is defined by the combination of yield and cropland area: S-O (optimistic, $S_{2100} = 1200$ Mt) assumes that the yield potential of 10,000 kg/ha is attained and the cropland red line of 120 million ha is maintained, S-M (medium, 1030 Mt) assumes a climate impact of -10% together with a 5% breach of the red line, and S-P (pessimistic, 860 Mt) a climate impact of -20% together with a 10% breach.

In what follows, the case P2 $\times$ D-M $\times$ S-O, which places an intermediate assumption on each of the population, demand, and supply axes (#13 of Toyohara and Zhou [2]), is referred to as the reference case, or baseline. The optimistic S-O is adopted on the supply axis so that the additional yield gain from AI-based precision agriculture (S-O+ in Section 3.2) is defined as an increment above the ceiling of the existing yield potential, thereby avoiding double counting.

It is useful to state at the outset on which case each of the results reported here is evaluated. The reference gap G_{ref} in Equation (3), the effect magnitudes of the five pathways, the waterfall decomposition, and the SRE trajectories reported in Section 3.4 are all evaluated

on the reference case. The effect magnitudes depend on that case because the three demand-side pathways scale with the population P_t and the demand trajectory: FCR improvement (Pathway (2)) is computed from a meat consumption of $m_{2100} = 90$ kg/person/year (D-M) and industrial AI (Pathway (3)) from $C^*_{2100} = 780$ kg/person/year (D-M), both multiplied by the 460 million of P2, while on the supply side precision agriculture (Pathway (4)) applies ρ_{PA} to $S_{2100} = 1200$ Mt (S-O). To isolate the dependence on population size, Section 3.2 instead compares P1, P2, and P3 while holding D-M × S-O fixed. Since the demand-side effects rise and fall in proportion to population, the maturity value SRE_∞ under full deployment is 0.44–0.90 under P1 and 0.62–1.10 under P3, so that under P3 the relaxation capacity of AI exceeds the reference gap. Beyond this, Section 3.5 solves all 27 scenarios for the year of self-sufficiency and the surplus thereafter, bounded by the most favorable case P1 × D-L × S-O (self-sufficiency in 2039, a surplus of 992 Mt in 2100) and the least favorable case P3 × D-H × S-P (2079 and 265 Mt), and shows that the effect of AI grows as the scenario becomes more demanding. The central conclusions of this study therefore do not hinge on the choice of the reference case.

The analysis period (2020–2100) is divided into two stages according to the nature of the underlying data.

For the observed-data period (2020–2024), key indicators—including the pig feed conversion ratio (FCR ≈ 3.0), the on-farm storage loss rate (≈ 3%), the precision-agriculture adoption area, and food-balance-sheet indicators ($C^*_{2024} = 590$ kg/person/year)—are drawn from observed records of the NBS, the Food and Agriculture Organization of the United Nations (FAO), and FAOSTAT and serve as the initial values and calibration anchors for the model. For the scenario-projection period (2025–2100), the 27-scenario system of Toyohara and Zhou [2] (Table 3) is used as the baseline, and the additional effects of AI technology across the five pathways are layered on top to quantify the SRE.

This two-stage design ensures that the observed values for 2020–2024 serve as confirmed benchmarks fixed prior to AI adoption. Every projected trajectory therefore starts from the same observed base, reported in the first column of Table 3 for 2020 (a population of 1412 million, a grain-equivalent consumption C^* of 583 kg/person/year, and a domestic supply of 669 Mt). The trajectories themselves are anchored at 2000 and at the 2024 observations ($C^*_{2024} = 590$ kg/person/year and a total grain output of 706.5 Mt). Scenario branching occurs only after this common observed starting point.

2.2. Demand-Side Effect Pathways

Demand-side effects arise through pathways such as labor displacement, FCR improvement, and industrial AI optimization. These are formalized in turn below. First, labor displacement by AI robots affects urban and rural workers, whose consumption structures differ. The weighted average displacement rate Q_L across workers is defined as

$$Q_{L,t} = \frac{\alpha R_{\text{urban},t} + \beta R_{\text{rural},t}}{\alpha + \beta} \tag{6}$$

where $R_{\text{urban},t}$ is the urban labor displacement rate, $R_{\text{rural},t}$ is the rural labor displacement rate, $\alpha = 0.67$ (urbanization-rate weight), and $\beta = 0.33$ (rural weight).

The decline in activity level accompanying this labor displacement also reduces demand. The occupational transition from manual labor to sedentary or less physically demanding work reduces food demand through lower energy expenditure. This effect is formalized as

$$\Delta D^{\text{AI}}_{\text{act},t} = N_{d,t} \times \gamma \times \Delta c^*_{\text{act}}, \qquad N_{d,t} = Q_{L,t} \times L_{\text{ag}} \tag{7}$$

where $N_{d,t}$ is the displaced population, obtained by applying the displacement rate $Q_{L,t}$ to a workforce base $L_{\text{ag}} \approx 260$ million—the manual-labor workforce across agriculture,

manufacturing, construction, and logistics, at its present-day level, and scaled with P_t in the projections—rather than to the total population P_t (displacement occurs within the workforce, whereas P_t includes non-working cohorts), so that the displaced population, and hence the demand-side effects, remain proportional to P_t; $\gamma \in [0,1]$ is the social safety-net sufficiency coefficient ($\gamma = 1$ is the upper bound at which full consumption transfer is realized), and Δc^*_{act} is the per-capita reduction in grain-equivalent consumption from the change in activity level (kg/year), obtained by converting the reduction in meat consumption Δm_{act} (5–7 kg/person/year; Section 3.1) into feed grain through the feed conversion ratio: $\Delta c^*_{\text{act}} = \Delta m_{\text{act}} \times \varphi_0$. Note, however, that since displaced workers continue to consume food after AI adoption ($\Delta P_t = 0$), this demand reduction is confined to the marginal contraction from lower activity levels.

The largest demand-side pathway is the improvement of the feed conversion ratio (FCR) through precision livestock AI, which directly reduces feed grain demand:

$$\Delta D^{\text{AI}}_{\text{fcr},t} = P_t \times m_t \times (\varphi_0 - \varphi_{\text{AI},t}) \tag{8}$$

where m_t is per-capita meat consumption (kg/year), $\varphi_0 = 3.0$ is the 2100 baseline pig-representative FCR (long-term convergence value, kg feed/kg meat), and $\varphi_{\text{AI},t}$ is the AI-adjusted FCR. Following the D-M scenario of Toyohara and Zhou [2], meat consumption m_t is assumed to reach 90 kg/person/year by 2100 (approximately 20% above the current level of 75 kg/person/year, supply basis). The estimated effect magnitude is presented in Section 3.1.

The AI optimization effect on the production process for industrial grain (based on this study's assumption that narrowly defined industrial use accounts for about 14% of C^*) is formalized as

$$\Delta D^{\text{AI}}_{\text{ind},t} = P_t \times C^*_{\text{ind},t} \times \eta_{\text{ind}} \tag{9}$$

where $C^*_{\text{ind},t}$ is per-capita industrial grain consumption (approximately $C^*_{2100} \times 0.14 \approx$ 109 kg/person/year under the 2100 D-M baseline), and $\eta_{\text{ind}} = 0.05$–0.10 is the input-efficiency improvement rate from AI optimization.

When, in addition, AI disease prediction and early intervention reduce livestock mortality, the effective FCR declines toward the biological FCR. The effective FCR accounting for the mortality rate m_d is defined as

$$\text{FCR}_{\text{eff}} = \frac{\text{FCR}_{\text{bio}}}{1 - m_d} \tag{10}$$

A decline in the mortality rate m_d lowers the effective FCR by improving slaughter output relative to feed input.

2.3. Supply-Side Effect: The S-O+ Scenario

The S-O scenario of Toyohara and Zhou [2] (2100 supply $S_O = 1200$ Mt) is a natural convergence trajectory that does not incorporate the proactive contribution of AI precision agriculture. Introducing the AI-enabled additional yield improvement rate ρ_{PA}, we define the S-O+ scenario as

$$S^+_{2100} = S_{O,2100} \times (1 + \rho_{\text{PA}}), \quad \rho_{\text{PA}} = 0.02\text{–}0.06 \tag{11}$$

We adopt the conservative midpoint $\rho_{\text{PA}} = 0.04$ as the representative value ($S^+_{2100} = 1200 \times 1.04 = 1248$ Mt; the estimated supply magnitude is presented in Section 3.2).

2.4. Key Parameter Justification

The key parameters used in this study and their literature bases are summarized in Table 4.

Table 4. Key parameters and their bases.

Parameter	Symbol	Value	Basis/Reference
2100 baseline FCR	φ_0	3.0	Pig-representative value, used in the primary calculation of Equation (8); the full species-weighted average is 3.25 (Table 5). Consistent with the aggregate 2100 feed coefficient of 3.0 in Toyohara and Zhou [2]
AI-adjusted FCR	φ_{AI}	2.5	Set by this study as the cumulative effect of precision feeding, genomic breeding, and disease management (3.0 → 2.5, a 16.7% reduction; decomposition in Section 3.1, technical basis in Section 4.2)
Meat consumption (D-M, 2100)	m_{2100}	90 kg/p/yr	D-M scenario of Toyohara and Zhou [2]
Industrial-grain efficiency gain	η_{ind}	0.05–0.10	An assumed range of this study, taking the +10% fermentation gain from an artificial neural network coupled with particle swarm optimization [15] (sugarcane) as mechanistic evidence and extending it to starch processing
Precision-ag additional yield gain	ρ_{PA}	0.02–0.06	A conservative assumption, about one fourth to one fifth of the reported yield gains of 10–25% [5], reflecting China's already high yield base
Urban/rural weights	α/β	0.67/0.33	Urbanization rate of 67.0% at the end of 2024 [16]
Social safety-net coefficient	γ	0.7–0.9	Level of income compensation for displaced workers; an assumption of this study, linked to the deployment scenario (note to the deployment-scenario table in Section 3.4; sensitivity in Section 3.6)
Loss reduction (target)	ℓ	3% → 1.5%	Extrapolation from the Grain Security Project record (8% → 3%, National Food and Strategic Reserves Administration); loss scale from Gustavsson et al. [17]

Note: $\varphi_0 = 3.0$ is the pig-representative value and is the value adopted in the primary calculation of Equation (8), together with $\varphi_{AI} = 2.5$; it is not the species-weighted average, which is 3.25 (post-AI 2.72) as derived in Table 5. A parallel calculation with the weighted pair is reported in Section 3.1 and yields a slightly larger effect, so the pig-representative pair is the conservative choice. The post-AI FCR $\varphi_{AI} = 2.5$ is a baseline value, not a single fixed estimate. A sensitivity analysis over four levels ($\varphi_{AI} = 2.8$, 2.7, 2.6, and 2.5; $\Delta\varphi = 0.2$–0.5) is given in Section 3.6, which confirms that FCR improvement remains the largest demand-side pathway even at the most conservative level, $\varphi_{AI} = 2.8$.

Table 5. FCR by livestock species and weighted-average calculation (NBS 2023 composition).

Species	FCR (φ_0/2100)	FCR (AI-Adjusted)	Share (%)	Weighted FCR (φ_0)
Pig	3.0	2.5	60	1.80
Poultry	2.0	1.7	25	0.50
Cattle	7.0	5.8	10	0.70
Sheep	5.0	4.2	5	0.25
Weighted average	3.25	2.72	100	—

Note: The φ_0 column is the 2100 baseline FCR (the commercial-farm standard after 25 years of non-AI improvement: pig FCR 4.0 → 3.0). The post-AI FCR is the value assumed in this study for the cumulative effect of precision feeding [9] and genomic selection [10]: about 17% improvement for pigs and about 15–17% for the other species. For the calculation we adopt the pig representative values $\varphi_0 = 3.0$ and $\varphi_{AI} = 2.5$; this $\varphi_0 = 3.0$ is consistent with the 2100 feed coefficient (aggregate 3.0) of Toyohara and Zhou [2]. The FCR used here is feed per edible meat (carcass-weight basis), which differs from China's industry-standard feed-to-liveweight ratio by the dressing yield. The species-level FCRs are standard values in animal nutrition (FAOSTAT does not publish FCR coefficients).

Among these, the feed conversion ratio (FCR) is set from species-level values, whose weighted average is derived below. China's meat production (NBS 2023) comprises pork (60%), poultry (25%), beef (10%), and mutton (5%). The biological FCR of each species (standard values from the animal-nutrition literature) and the weighted values are presented in Table 5.

The FCR is assumed to improve in stages: from the 2024 national average (an effective average of ≈3.74, including small-scale farms and inefficient operations—a concept distinct from the commercial-farm species-weighted value of 3.25, and estimated in this study),

through convergence to the commercial-farm standard, reaching a 2100 baseline species-weighted FCR of 3.25 (pig FCR $\varphi_0 = 3.0$), and then, with the introduction of AI technology, improving to a species-weighted 2.72 (pig FCR $\varphi_{AI} = 2.5$) (Figure 1).

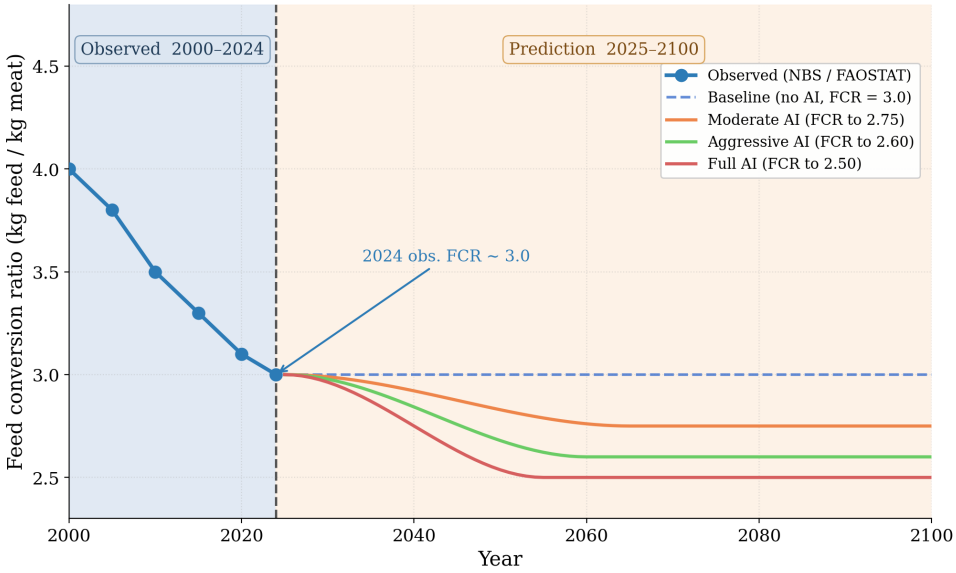


Figure 1. Observed FCR trajectory (2000–2024) and scenario projections (2025–2100). The observed pig FCR declines from about 4.0 to 3.0 over 2000–2024; AI deployment scenarios drive further improvement toward 2.75/2.60/2.50. The vertical dashed line (2024) marks the last year of observed data. Under the baseline (no AI) the FCR stays at 3.0 from 2025 onward, whereas under full deployment it converges to 2.5 by about 2055. The observed series is derived by us from feed use (FAOSTAT food balance sheets; 2024 extrapolated) and livestock output (NBS), and is not an FCR coefficient published by FAOSTAT. The projected curves show when each FCR level becomes technically attainable at scale; how much of that potential is realized in the SRE calculation at a given date is governed separately by the realization rate $A(t)$ of Equation (4). The blue shading marks the observed period (2000–2024) and the orange shading the projection period (2025–2100).

3. Results: Quantitative Assessment of Five Pathways

3.1. Effect 1: Relaxation of Feed Supply–Demand Pressure

The relaxation of feed supply–demand pressure begins with a decline in activity levels driven by labor displacement. China's urban manual laborers number on the order of 200 million (our order-of-magnitude reading of national employment statistics). When high-calorie-consuming workers engaged in manufacturing, construction, and port cargo handling are displaced by AI robots, their food consumption declines in proportion to the reduction in their activity level.

For urban adults in Beijing, occupational energy expenditure has been directly measured using the doubly labeled water method [18]. That study reports that both weight-adjusted total energy expenditure and the physical activity level rise with occupational category, and that the level of occupational activity, rather than leisure activity, significantly predicts total energy expenditure; it does not, however, report the size of the manual-to-sedentary difference, so the magnitude below is our own assumption informed by that finding. We take the transition from manual labor to sedentary or inactive states to lower energy expenditure by approximately 15–20%, which, converted to meat consumption, corresponds to a reduction of 5–7 kg/person/year (our conversion).

At the port of Tianjin (one of China's largest container ports), the deployment of automated guided vehicles (AGVs) and automated cranes has accelerated since the 2020s, and the automation rate of large container equipment has exceeded 88% [19]. Whereas

each shift on a conventional operating line previously required 9–10 workers for quay and yard cranes and trailers, at automated terminals the work is completed by 1–2 remote operators, and average operational efficiency is reported to have improved by 15% [19]. Such port automation illustrates that the displacement of manual labor is already under way in practice.

An estimate based on Equation (7) shows that, in a moderate scenario with 10 million displaced workers and a social safety-net coefficient $\gamma = 0.7$, the feed-grain-equivalent reduction amounts to only 0.11–0.15 Mt/year: $\Delta D_{\text{act}}^{\text{AI}} = 10^7 \times 0.7 \times (5\text{–}7\ \text{kg} \times 3.0) = 0.105\text{–}0.147$ Mt/year (Section 3.4). This figure is two orders of magnitude smaller than the FCR improvement effect discussed below (20.7 Mt/year at full deployment, where the like-for-like ratio is about 20-fold), and the food-demand contraction from labor displacement should not be overstated.

The largest relaxation on the demand side comes from FCR improvement through precision livestock AI. The starting point is the observed FCR record over 2000–2024. In China's commercial pig industry, the pig FCR is considered to have fallen from approximately 4.0 in the early 2000s to approximately 3.0 through selective breeding, improved compound feeds, and the spread of large-scale farming (3.0 kg of feed per kg of pork) by the early 2020s (a standard level in livestock nutrition, consistent with the 2100 feed conversion coefficient of 3.0 in Toyohara and Zhou [2]). This non-AI improvement of approximately 25% over 25 years is of the same order as the additional improvement from AI utilization assumed in this study (FCR 3.0→2.5, approximately 17% reduction), placing the projection in line with past technological progress. AI-driven FCR improvement proceeds through three pathways (precision feeding, genomic breeding, and disease prediction), which we examine in turn.

Precision feeding, through optimal individual-level control of feed quantity by IoT sensors and machine learning, eliminates overfeeding and achieves precise nutritional management. That precision feeding improves feed efficiency while reducing nutrient excretion and feed costs in pigs has been reported in both empirical and modeling studies [9]. Building on these findings, we assume an FCR improvement of 5–12% from precision feeding. Note that Gaillard et al. [9] report the effects of precision feeding in terms of nutrient-use efficiency, excretion, and feed cost rather than a quantified FCR reduction; the 5–12% used here is our own assumption informed by these mechanisms. As adoption spreads across China's commercial pig facilities (large-scale farms), an improvement of about 3–6% in the national average FCR can be expected.

Genomic breeding is the second pathway: combining genomic selection with AI-based breeding-value prediction raises the rate of feed-efficiency improvement compared with conventional breeding. Simulation studies of breeding programs show that genomic selection for pigs raises the annual monetary genetic gain by 9–12% relative to conventional (progeny-test) breeding, and raises the annual gain in the feed conversion ratio (FCR) alone by 7–15% [10]. If this technology diffuses in China's swine industry (the world's largest), the breeding effect will manifest after a lag of 10–20 years and cumulatively lower FCR over the long term.

The third pathway, disease prediction and early intervention, is evaluated through the mortality-rate adjustment of Equation (10). For commercial pigs (three-way crossbred; 6.13 million head) at a large Chinese pig-producing enterprise, the survival rate from weaning to marketing was reported at 90.6% in 2020 and 85.8% in 2021, i.e., mortality rates of 9.4% and 14.2% [20]. According to the mortality-rate adjustment of Equation (10), the change in the effective FCR value when a commercial-standard mortality level (e.g., 5%) is halved (to 2.5%) through AI disease prediction and early intervention is as follows.

$$\mathrm{FCR}_{\mathrm{eff}}(m_d = 0.05) = \frac{3.0}{1 - 0.05} = 3.16$$
$$\mathrm{FCR}_{\mathrm{eff}}(m_d = 0.025) = \frac{3.0}{1 - 0.025} = 3.08$$

This difference corresponds to an FCR improvement of approximately 2.6%. With the implementation of AI disease prediction, vaccination optimization, and early isolation, a further reduction in effective FCR is expected as industry-level mortality management improves.

As the cumulative effect of these three pathways, an FCR of 3.0 → 2.5 (a 16.7% reduction) is assumed to be an achievable level. The mechanisms are not independent but combine multiplicatively, so that $(1-a)(1-b)(1-c) = 2.5/3.0$, where a is the improvement from precision feeding, b from genomic breeding, and c from disease prevention. Setting a = 5–12% (as assumed above) and $c \approx 2.6\%$ (the effect of a mortality reduction from 5% to 2.5% by Equation (10)) implies a required contribution from genomic breeding of b = 2.8–9.9%. Lopez et al. [10] report that genomic selection raises the annual rate of FCR improvement by 7–15% relative to conventional breeding; when accumulated over the 75 years from 2025 to 2100, the value of b above is conservative. The allocation among the mechanisms is nonetheless an assumption of this study and requires empirical support. Under the 2100 D-M scenario (P2 = 460 million; $m_{2100} = 90$ kg/person/year), Equation (8) gives

$$\Delta D^{\mathrm{AI}}_{\mathrm{fcr},2100} = 4.60 \times 10^8 \times 90 \times (3.0 - 2.5) = 20.7\,\mathrm{Mt/year}$$

which, as shown in the synthesis table below, is the largest effect among the three demand-side (grain use efficiency) pathways. The primary calculation uses the pig-representative pair ($\varphi_0 = 3.0$, $\varphi_{\mathrm{AI}} = 2.5$). If the full species-weighted pair of Table 5 ($\varphi_0 = 3.25$, $\varphi_{\mathrm{AI}} = 2.72$; $\Delta\varphi = 0.53$ from the rounded post-AI value) is used instead, the same equation gives $4.60 \times 10^8 \times 90 \times 0.53 = 21.9$ Mt/year, about 6% larger. The pig-representative pair is therefore the conservative choice, and neither the ranking of the pathways nor any conclusion of this study depends on which pair is adopted.

Under the population-target scenario (P3 = 700 million), the same equation gives

$$\Delta D^{\mathrm{AI}}_{\mathrm{fcr},2100}\,(\mathrm{P3} \times \mathrm{D\text{-}M}) = 7.00 \times 10^8 \times 90 \times (3.0 - 2.5) = 31.5\,\mathrm{Mt/year}$$

which is 1.52 times the P2 reference value (20.7 Mt/year). Because feed grain demand also grows under P3 as the livestock industry expands in scale, the absolute effect of FCR improvement is larger than under P2, further raising the policy priority of precision livestock AI.

AI optimization of industrial processes also reduces the demand for industrial grain. The C^* end-use breakdown in Toyohara and Zhou [2] reports industrial/other use (bioethanol, starch sugar, seed, loss, and statistical residual) as a single aggregate: 165 kg/person/year in 2024 (about 28% of C^*) and 370 kg/person/year in 2100 under D-M. Because that study does not separate narrowly defined industrial use, this study assumes narrow industrial use (excluding seed, loss, and the statistical residual) to be about 14% of C^* (about 83 kg/person/year on a 2024 empirical basis). Its composition is starch processing (approximately 50%), alcohol and ethanol production (approximately 32%), and food additives and others (approximately 18%) (approximate industry structure; the shares vary by year roughly within 50–55%/26–32%/18–19%).

Because the consumption of industrial grain is determined by output volume and policy rather than by the number of workers, the direct effect of labor displacement is zero. However, AI optimization of fermentation, enzymatic reactions, and manufacturing processes improves raw-material input efficiency. For an industrial ethanol plant (sugarcane, Brazil), combining artificial neural networks (ANN) with particle swarm optimization

(PSO) has been shown to raise the ethanol concentration and output at the end of fermentation by about 10% [15]. Because China's industrial grain (corn deep-processing) uses a different feedstock, we invoke this result as mechanistic evidence for AI optimization of fermentation processes rather than as a directly transferable magnitude. Comparable applications have now been reported for China's own corn-processing chain, in which glucose-derived L-lysine is a major product: a Chinese study coupling an artificial neural network with a genetic algorithm to control L-lysine fermentation achieved a peak titer of about 213 g/L [21], and machine-learning-guided optimization of corn-straw ethanol fermentation has been validated experimentally [22] (corn stover, a lignocellulosic feedstock). These studies demonstrate the mechanism on Chinese feedstocks, although they report optimization capability rather than an industry-wide efficiency rate; $\eta_{\text{ind}} = 0.05$–0.10 therefore remains an assumption of this study, and its full range moves the maturity SRE by about 0.02 (Section 3.6).

For the 2100 D-M scenario, with a representative value of $\eta_{\text{ind}} = 0.08$ within the assumed range 0.05–0.10, Equation (9) gives

$$\Delta D^{\text{AI}}_{\text{ind},2100} = 4.60 \times 10^8 \times 109 \times 0.08 \approx 4\,\text{Mt/year}$$

which is about one-fifth of the FCR improvement (20.7 Mt/year).

3.2. Effect 2: Supply Maintenance and Enhancement via Precision Agriculture

On the supply side, agricultural AI robots first prevent farmland abandonment and thereby help sustain the S-O scenario. The observed adoption of precision agriculture technologies is as follows. The application area of agricultural drones (unmanned aerial vehicles, UAVs) has expanded rapidly since the pilot-introduction phase in the mid-2010s: the annual cumulative operational area reached 2.13 billion mu-times (about 142 million ha) in 2023 [4] and 2.67 billion mu-times (about 178 million ha, with a fleet of 251,000 units) in 2024 [14]. Both are aggregates that include overlapping applications, so the cropland actually covered is a subset thereof, and no official statistic for the unique coverage rate is published. Large-scale farming enterprises have likewise been building out digital data-management systems over the past decade e.g., [20], and this diffusion trajectory forms the technological and infrastructure foundation for broad deployment from 2030 onward.

Advancing rural aging and depopulation create farmland abandonment risks due to labor shortages. The risk is empirically substantial. Global mapping reports 8.7 million ha for China over 1992–2020, behind Russia (12.4 million ha) and ahead of Brazil (8.4 million ha) [23], and a machine-learning assessment, using a broader detection approach than the long-term mapping, estimates that 31.2 million ha were abandoned as of 2022, of which about 83% is judged suitable for recultivation with a potential grain gain of roughly roughly 162 Mt per year [24]. The mechanisms are also documented: household-level evidence shows that farmland fragmentation raises the probability of abandonment partly by constraining mechanization [25], and city-level evidence from southern China finds abandonment concentrated in mountainous and hilly terrain, with potential crop yield, soil properties, mean annual precipitation, population density, and terrain features among the main drivers [26]. Meanwhile, evidence from the Yangtze River Economic Belt shows grain output rising even as cultivated land shrinks in area and degrades in quality in most of the cities studied, an offset sustained by intensified fertilizer, machinery, and electricity inputs, and judged unsustainable [27], which makes the preservation of effective cropland, rather than further input intensification, the binding constraint. Cropland fell from 130 million ha in 2000 to 128 million ha in the Third National Land Survey (2020) and then recovered to 129.3 million ha by the end of 2024, leaving a 7.7% margin above the red line (120 million ha) [2]. This margin is nonetheless under downward pressure

from urbanization, desertification, and labor shortages, and the S-P (pessimistic) scenario assumes a 10% reduction from the red line (108 million ha).

The rural diffusion of AI robots (driverless tractors, automated harvesters, drone sprayers) prevents labor-shortage-driven abandonment and raises the feasibility of the S-O (optimistic) scenario (120 million ha maintained). The difference in supply between S-O and S-P is 340 Mt (1200 − 860 Mt). Not all of this difference can be attributed to AI. It bundles two distinct assumptions of the S-P trajectory: a climate impact of −20% on yields (≈240 Mt) and a 10% breach of the cropland red line (≈120 Mt), less their interaction (≈24 Mt); the small remainder is rounding in the published trajectories. Agricultural AI robots can act only on the cropland component, and within it only on the share of the loss that is driven by labor shortage rather than by land conversion or degradation. The 340 Mt is therefore the ceiling of the whole trajectory shift, of which the abandonment-prevention contribution attributable to AI is a fraction, plausibly on the order of 100 Mt at most. This is why pathway (4b) is treated throughout as a conditional, qualitative upside and is excluded from the SRE accounting.

Beyond preventing farmland abandonment, AI precision agriculture also raises yields directly (the S-O+ scenario). The S-O scenario is a natural convergence trajectory in which yield growth decelerates from the observed 2000–2024 compound annual growth rate of +1.36%/year toward the yield potential of 10,000 kg/ha, with production growth falling from +1.0%/year in 2025–2050 to +0.4%/year in 2075–2100 [2].

A systematic review [5] compiles (in Table 1 of that review) reported gains of 10–25% in yield for real-time crop monitoring combining drones, satellite imagery, and IoT sensors, and of 15–30% for GPS-guided optimization of sowing and harvesting. These figures, however, summarize individual reports from diverse fields and countries and cannot be extrapolated directly to China's intensive agriculture, where yields are already high and mechanization and irrigation infrastructure are in place. Field evidence from China itself points in the same direction: an econometric study of 520 rice growers in mountainous Yunnan finds that plant-protection UAV adoption cut pesticide expenditure by 77.3 CNY/mu and raised rice yields by 196.9 kg/mu [28], and wheat field trials report control efficacy of about 71% at seven days—below that of boom and mist-blower sprayers, though achieved at 1.7 and 2.6 times their respective working efficiencies, and at 20 times that of a knapsack sprayer [29]. The Yunnan estimates are averages: the same study finds the yield gain concentrated among growers with larger and more fertile plots, so the effect on smaller or more marginal holdings is smaller than the mean. We therefore assume an additional yield gain of $\rho_{\mathrm{PA}} = 2$–6%, a level well below the lower bound of these reported ranges.

Substituting $\rho_{\mathrm{PA}} = 0.04$ (midpoint) into Equation (11):

$$S^{+}_{2100} = 1200 \times 1.04 = 1248\,\mathrm{Mt}$$

Under the P2 × D-M scenario (the baseline of Toyohara and Zhou [2]), the food surplus expands from 841 Mt (S-O basis) to 889 Mt (S-O+ basis). For the worst case (P3 × D-H × S-P), the improvement is from 265 Mt to 299 Mt. S-O+ is treated as an "optimistic upside" rather than the central scenario; S-O remains the reference scenario.

Both the AI effects and the food surpluses depend on population scale. Table 6 presents the FCR improvement effects and food surpluses across the three population scenarios P1, P2, and P3, and Figure 2 illustrates the surplus by AI deployment level.

Table 6. AI effect magnitudes and food surplus by population scenario (2100; D-M × S-O as the central reference).

Indicator	P1 (320 M)	P2 (460 M)	P3 (700 M)
FCR improvement effect (Mt/year)	14.4	20.7	31.5
Industrial AI reduction (Mt/year)	2.8	4.0	6.1
Food surplus: D-M×S-O (Mt)	950	841	654
Food surplus: D-M×S-O+ (Mt)	998	889	702
Food surplus: worst D-H×S-P (Mt)	588	469	265
Maturity SRE_{∞} (full deployment)	0.44–0.90	0.51–0.97	0.62–1.10

Note: The demand-side effects (labor displacement, FCR improvement, and industrial AI) scale with population (obtained by multiplying the P2 reference by P3/P2 = 1.52 and P1/P2 = 0.70). Supply-side effects (precision agriculture, loss reduction) are production-based and do not scale with population. Because SRE_{∞} is normalized by the fixed reference gap G_{ref} = 112 Mt, it varies with the population scenario; under P3 the relaxation capacity of AI exceeds the reference gap (SRE > 1). Food surplus = $S - D$ ($D = P \times C^{*}_{2100}$). A food surplus is confirmed in all 27 scenarios, and under P3 the absolute magnitude of FCR improvement is 1.52 times the P2 value.

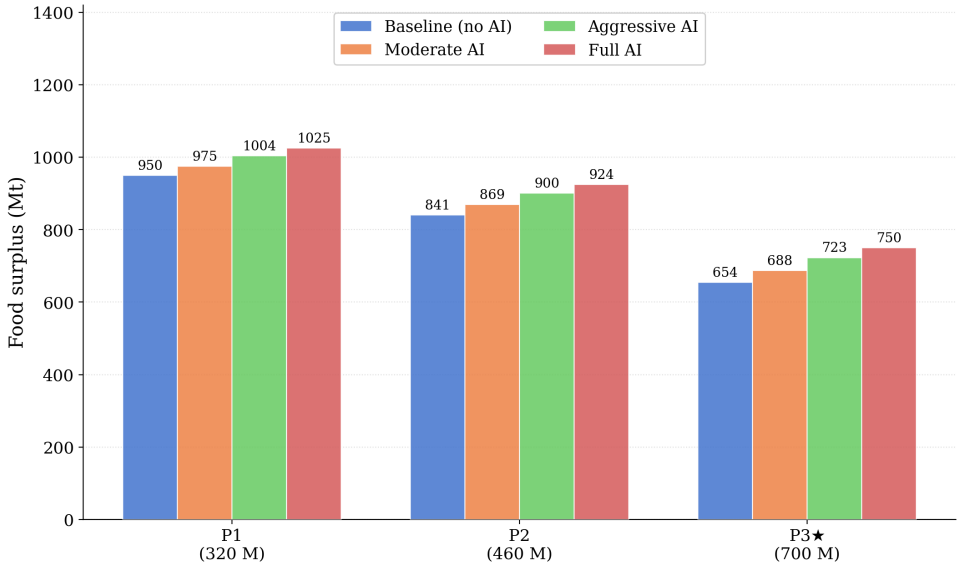


Figure 2. Food surplus in 2100 by population scenario and AI deployment level (D-M × S-O basis). Baseline surpluses are from Toyohara and Zhou [2]; the AI increment is the sum of the demand-side effects (labor displacement, FCR improvement, and industrial AI), which scale with population, and the supply-side effects (S-O+ precision agriculture and loss reduction), which do not. Each bar uses the midpoint of the effect range of each pathway. A surplus is maintained across all scenarios and deployment stages, and AI adoption expands the surplus even in the worst P3 case. ★ P3 = birth-rate-support policy target (TFR ≈ 1.31; 700 million in 2100).

3.3. Effect 3: Post-Harvest Loss Reduction via AI Storage and Inventory Management

The trend in China's grain post-harvest loss over 2000–2024 is as follows. International estimates of food loss place the post-harvest handling and storage loss rate for cereals at approximately 10% in industrialized Asia (approximately 12% when the agricultural production stage is included) [17]. China's grain loss was also close to this level in the early 2000s, at approximately 8% (the Grain Security Project's baseline, corresponding to roughly 40 Mt per year at the production scale of that period), but in 2012 the Chinese government began full-scale promotion of the "Grain Security Project" (*liang an gong cheng*), implementing the modernization of rural warehouses, the development of drying facilities, and the diffusion of low-temperature storage technology on a nationwide scale. Through roughly a decade of these efforts, the loss rate was reduced by about 62%, with farm-level storage losses falling to approximately 3% and state-owned warehouse losses to below

1% by the early 2020s (National Food and Strategic Reserves Administration; an observed improvement achieved through non-AI technology).

The residual loss volume is as follows.

$$\text{annual loss} \approx 700\,\text{Mt} \times 3\% \approx 21.0\,\text{Mt/year}$$

AI/IoT-based dynamic temperature-humidity control of the storage environment, optimization of inventory rotation, and enhanced logistics planning can further reduce losses at the storage and transport stages. This study sets a target of reducing the loss rate from the current 3% to 1.5%. This reduction (1.5 percentage points) is only 30% of the 8%→3% (5 percentage points) already achieved by the non-AI Grain Security Project, and is thus a conservative assumption. Accordingly, the incremental supply gain, depending on the production base, would be roughly 9.0–10.5 Mt/year, the range reflecting whether the 1.5-point reduction is applied to the whole of current output (≈700 Mt) or only to the share that passes through on-farm and commercial storage, while the portion actually realized under moderate AI deployment is about 2.7–3.15 Mt/year (consistent with the synthesis table in the following section).

3.4. Integrated Quantitative Analysis

Among the three demand-side pathways, FCR improvement clearly exceeds the others (Figure 3). On the supply side, precision agriculture (4) has the largest effect magnitude, but this operates through a different mechanism, namely additional production.

Figure 3 traces how the five pathways draw down the 2030 baseline supply–demand gap of 112.26 Mt, with the pathway effects subtracted in descending order of magnitude. The pathway contributions are 48 Mt for precision agriculture (4), 20.7 Mt for FCR improvement (2), 9.75 Mt for loss reduction (5), 3.75 Mt for industrial AI (3), and 0.97 Mt for labor displacement (1); the top two pathways alone account for 83% of the total relaxation. The five pathways together relax 83.17 Mt of the gap, leaving a residual gap of $112.26 - 83.17 = 29.09$ Mt and an SRE of $83.17/112.26 = 0.74$, which lies within the full-deployment range of 0.51–0.97. The ranking by effect magnitude does not, however, coincide with the priority ranking for public investment. Precision agriculture is a conditional effect premised on the optimistic S-O supply and diffuses through market forces, whereas FCR improvement does not depend on the supply scenario, and the genomic breeding at its core is rate-limited by generational turnover and thus requires public research and development with a long horizon (Section 4.4). Prevention of farmland abandonment by AI robots (pathway (4b), an S-P → S-O trajectory shift whose AI-attributable share is on the order of 100 Mt at most, Section 3.2) is a conditional upside and is excluded from the figure.

As Table 7 shows, FCR improvement yields the largest effect on the demand side, one to two orders of magnitude larger than labor displacement (Pathway (1)).

We define the deployment scenario as the policy and investment choice of how broadly and how intensively China adopts AI. It comprises three levels (moderate, aggressive, and full) and is defined, for each of the five pathways, as a realization rate relative to full deployment (100% of the technical potential; Table 8). FCR improvement (Pathway (2)) depends not on the level of livestock technology as such but on the uptake of precision feeding and the scale of genomic breeding programs, and is therefore defined by a realization rate in the same way as the other four pathways. The maturity SRE_∞ spans roughly a threefold range across deployment scenarios (0.18–0.32/0.37–0.69/0.51–0.97); the increase from the moderate to the full upper bound decomposes into precision agriculture 68%, FCR improvement 14%, loss reduction 10%, industrial AI 6%, and labor displacement 1%, so the two supply-side pathways account for about 80% of it. The deployment scenario sets only the ceiling of the effect; the number of years needed to reach that ceiling is governed

separately by the diffusion scenario (Table 2), and the uncertainty in the magnitude of the FCR improvement itself by the FCR sensitivity analysis (Section 3.6). The two are related as a target level and its degree of attainment: the realized effect at any date is their product, $\mathrm{SRE}_{\infty}(\text{deployment}) \times A(t;\ \text{diffusion})$, so a single-date observation cannot separate them—full deployment at $A = 0.17$ and moderate deployment at maturity both correspond, for example, to a displaced population of about 10 million, although the former keeps rising toward 60 million while the latter stops there. Realization rates differ across pathways because of differences in technical characteristics: precision agriculture can be procured as an outsourced service at a low capital barrier and loss reduction requires only the retrofitting of existing infrastructure, whereas industrial AI requires equipment renewal and labor displacement requires large-scale replacement of agricultural machinery. The drivers of the five pathways are likewise distinct: precision agriculture depends on the market for drone spraying services, loss reduction on the retrofitting of warehouse and cold-chain infrastructure, industrial AI on the capital-investment decisions of grain processors (mostly state-owned), labor displacement on the replacement of agricultural machinery, and FCR improvement on the uptake of precision feeding and the progress of genomic breeding. The actors, the capital requirements, and the time scales all differ, so there is no reason for them to move in step. The deployment scenario is therefore a compound scenario that bundles five independent technological domains under the single narrative of national AI investment intensity; it is not a single physical parameter. The consequences of the pathways moving independently are examined by a bounding check in Section 3.6.

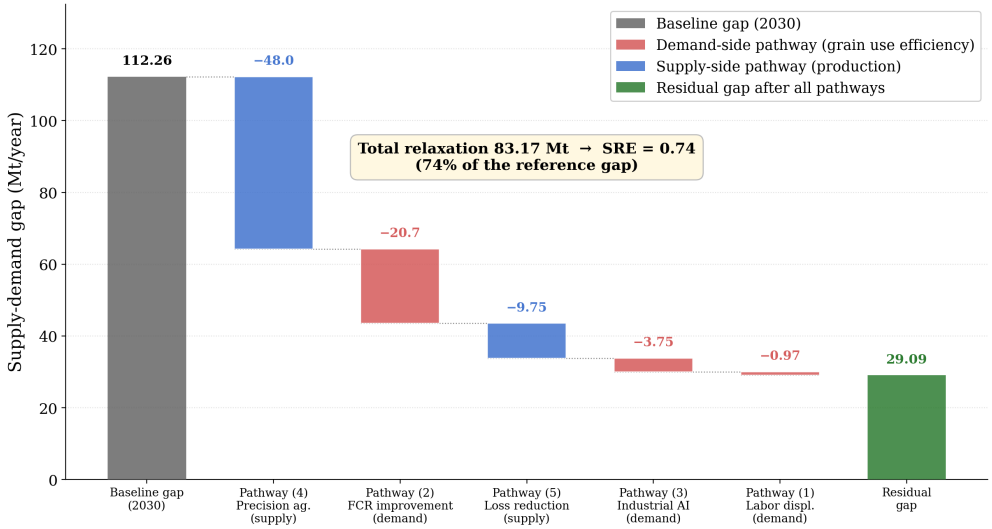


Figure 3. Process by which the five AI pathways relax the supply–demand gap. Assumptions: the baseline case (population P2 × demand D-M × supply S-O; Table 3), full deployment, the reference FCR scenario (post-AI FCR = 2.5, $\Delta\varphi = 0.5$), $\rho_{\mathrm{PA}} = 4\%$ (central), and maturity ($A \to 1$). Red denotes the demand side (improved grain use efficiency) and blue the supply side (increased production). All values are computed against the precise reference gap $G_{\mathrm{ref}} = 112.26$ Mt (Equation (3)). The bars for precision agriculture, loss reduction, industrial AI, and labor displacement are the midpoints of their effect ranges; the FCR bar is the value at the baseline $\Delta\varphi = 0.5$. Midpoints are taken over the ranges as printed in Table 8. Grey bar: baseline gap in 2030; red bars: demand-side pathways; blue bars: supply-side pathways; green bar: residual gap after all five pathways. The labels in parentheses indicate the side (demand or supply) on which each pathway acts. Negative values are the reductions of the gap in Mt/year.

Table 7. Effect magnitudes of the five pathways (technical potential of each pathway).

Pathway	Direction	Annual Effect (Mt/Year)
Demand side (improvement in grain use efficiency)		
(1) Activity-level decline from labor displacement	Demand ↓	0.81–1.13
(2) FCR improvement via precision livestock AI	Demand ↓	20.7–31.5
(3) AI optimization of industrial processes	Demand ↓	≈4
Supply side (production increase)		
(4) Yield improvement via precision agriculture (S-O+)	Supply ↑	24–72
(5) Loss reduction via AI inventory management	Supply ↑	9.0–10.5

Note: ↓ denotes a demand-side reduction and ↑ a supply-side increase. All effect magnitudes are our estimates (by Equations (7)–(11)). The references for each pathway's technical mechanism are: (1) labor displacement Yao et al. [18]; (2) FCR improvement Gaillard et al. [9] (precision feeding), Lopez et al. [10] (genomic breeding), and Halachmi et al. [8] (sensor infrastructure); (3) industrial AI Pereira et al. [15]; and (4) precision agriculture Getahun et al. [5]. For (5) loss reduction, the reference levels for the scale and stage-wise breakdown of losses are taken from Gustavsson et al. [17] (industrialized Asia, cereals: 10% at post-harvest handling and storage) and the observed reduction from the National Food and Strategic Reserves Administration (Grain Security Project, 8% → 3%); the additional reduction through AI inventory management (3% → 1.5%) is an assumption of this study. The demand side corresponds to improved grain use efficiency and the supply side to increased production. Pathway (4) is the additional yield gain from precision agriculture (ρ_{PA} = 2–6%; S-O 1200 → S-O+ 1224–1272 Mt), counted in the main S-O-based analysis. FCR improvement (2) emerges gradually over 2030–2050 and reaches about 20.7 Mt/year (P2) by 2100. Pathway (4b) (prevention of farmland abandonment) is a conditional upside and is not counted in this table (Section 3.2).

On this basis, Table 8 sets out the realization rate and the effect magnitude of each pathway under each deployment scenario.

Integrating the five pathways, we obtain the supply-side effect at maturity ($A \to 1$), $\Delta S_{\infty}^{\mathrm{AI}}$, as the sum of the yield increase from precision agriculture (Pathway (4)) and post-harvest loss reduction (Pathway (5)). Here, Pathway (4) is realized in proportion to the deployment range of precision agriculture (its coverage as a share of total cropland): of its full technical potential (24–72 Mt/year, corresponding to ρ_{PA} = 2–6%), we assume that approximately 30% is realized under moderate deployment (7.2–21.6), approximately 70% under aggressive deployment (16.8–50.4), and 100% under full deployment (24–72). Post-harvest loss reduction (5) manifests early through improvements to existing infrastructure and therefore attains a relatively high realization rate (moderate 2.7–3.15, aggressive 6.75–7.88, full 9.0–10.5 Mt/year; Table 8). As the sum of the two, $\Delta S_{\infty}^{\mathrm{AI}}$ is 9.90–24.75 Mt/year under moderate deployment, 23.55–58.28 under aggressive deployment, and 33.0–82.5 under full deployment (on the S-O basis; farmland abandonment prevention (4b) is not counted, as it is a conditional effect). The demand-side effect $\Delta D_{\infty}^{\mathrm{AI}}$ is the sum of pathways (1), (2), and (3): 10.71–11.00 (moderate), 17.92–19.07 (aggressive), and 24.02–26.86 Mt/year (full). FCR improvement (2) emerges with the uptake of precision feeding and genomic breeding, so the post-AI FCR is 2.75, 2.60, and 2.50, giving 10.35, 16.56, and 20.70 Mt/year, respectively. Substituting these into Equation (3) and using the fixed reference gap G_{ref} = 112 Mt (the 2030 baseline gap, computed from Table 3) as the denominator, the SRE at maturity, SRE_{∞}, is 0.18–0.32 for moderate, 0.37–0.69 for aggressive, and 0.51–0.97 for full deployment. Under full deployment the upper bound reaches SRE_{∞} = 0.97, meaning that the relaxation capacity of AI is of almost the same magnitude as the reference gap (112 Mt in 2030). This does not mean that the future supply–demand gap is closed; the actual timing of self-sufficiency and the effect on the surplus thereafter are presented in Section 3.5. Note that SRE_{∞} is a value at maturity ($A \to 1$), not the effect realized in 2030. Under central diffusion the adoption rate in 2030 is only $A(2030)$ = 0.40, so the SRE realized in that year is 40% of the maturity value (Table 9). The reduction in the medium-term (2030) import dependence of 12–14% is accordingly limited to 0.9–1.6 percentage points under moderate deployment, 1.9–3.5 points under aggressive deployment, and 2.6–5.0 points even under full deployment. The maturity value SRE_{∞}, by contrast, measures the magnitude of

the relaxation capacity relative to the 2030 reference gap; it is not a statement about import dependence in the year of maturity. By 2100, population decline will already have delivered self-sufficiency (Section 3.5), so import dependence no longer exists.

Realizing the maturity level, however, takes time. The SRE in any given year is $\mathrm{SRE}_t = \mathrm{SRE}_\infty A(t)$ and is therefore determined by the combination of the deployment scenario (the ceiling of the effect) and the diffusion scenario (the timing of its realization). All nine combinations are shown in Table 9, and the trajectories for all three diffusion scenarios in Figure 4. As Figure 4 shows, the maturity level (0.18–0.32/0.37–0.69/0.51–0.97) does not depend on the diffusion scenario, and the 2100 value differs only marginally across scenarios. Even under full deployment with central diffusion, the SRE in 2030 remains at 0.20–0.39. The level realistically attainable by then is that of moderate deployment, SRE 0.07–0.13. The rightmost column is identical across diffusion scenarios: by construction, the maturity value SRE_∞ does not depend on the diffusion speed.

Table 8. Definition of the deployment scenarios: realization rates and effect magnitudes by pathway.

Pathway/Parameter	Moderate	Aggressive	Full
Realization rate (relative to full deployment = 100% of technical potential)			
(4) Precision agriculture (cropland coverage)	30%	70%	100%
(5) Loss reduction	30%	75%	100%
(2) FCR improvement (precision-feeding/breeding uptake)	50%	80%	100%
(3) Industrial AI optimization	10%	40%	100%
(1) Labor displacement	13%	44%	100%
Effect magnitude (Mt/year, at maturity $A \to 1$)			
(4) Precision agriculture (supply)	7.2–21.6	16.8–50.4	24.0–72.0
(5) Loss reduction (supply)	2.7–3.15	6.75–7.88	9.0–10.5
ΔS^{AI} total	9.90–24.75	23.55–58.28	33.0–82.5
(2) FCR improvement (demand) *	10.35	16.56	20.70
(3) Industrial grain reduction (demand) §	0.25–0.50	1.0–2.0	2.5–5.0
(1) Feed grain reduction (demand)	0.11–0.15	0.36–0.50	0.81–1.13
ΔD^{AI} total	10.71–11.00	17.92–19.07	24.02–26.86
Maturity SRE_∞	0.18–0.32	0.37–0.69	0.51–0.97
Breakdown of labor displacement			
Displaced population (millions) †	10	30	60
Meat consumption reduction (Mt/year)	0.035–0.049	0.12–0.17	0.27–0.38
Social-security coefficient γ ‡	0.7	0.8	0.9

Note: Pathway numbers (1)–(5) follow Table 7. Realization rates are expressed relative to full deployment (100% of the technical potential). They differ across pathways because of differences in technical characteristics (Section 3.4). $\mathrm{SRE}_\infty = (\Delta S^{\mathrm{AI}} + \Delta D^{\mathrm{AI}})/|G_{\mathrm{ref}}|$ with $G_{\mathrm{ref}} = 112.26$ Mt (2030, P2 × D-M × S-O; see Section 2.1). * FCR improvement emerges with the uptake of precision feeding and genomic breeding, so the post-AI FCR is 2.75 (moderate), 2.60 (aggressive), and 2.50 (full) (Figure 1). The effect is $P \times m \times \Delta\varphi$ with $P = 460$ million and $m = 90$ kg/person/year. § The industrial-AI effect is computed from Equation (9) ($P \times C^*_{\mathrm{ind}} \times \eta_{\mathrm{ind}}$, with $C^*_{\mathrm{ind}} = 109.2$ kg/person/year and $\eta_{\mathrm{ind}} = 0.05$–$0.10$) multiplied by the realization rate. † The displaced populations shown here are the P2 values. The displacement rate Q_L (0.038/0.115/0.231) is obtained by dividing them by the P2 manual-labor workforce (agriculture, manufacturing, construction, and logistics) of approximately 260 million, and is then held fixed across population scenarios; the workforce, and hence the displaced population, scales with P_t, which is why the demand-side effects are proportional to population in Table 6. ‡ γ is in principle a redistribution-policy variable independent of the breadth of AI adoption; we link it to the deployment scenario on the assumption that a government undertaking large-scale labor displacement is compelled to strengthen social security (sensitivity in Section 3.6).

Because $A(2100)$ is 1.00 under early diffusion, 0.99 under central, and 0.97 under late, the SRE in 2100 is 97–100% of the maturity value (0.49–0.94, for instance, under full deployment with late diffusion). What matters for policy is the level attained during the transition, which is why the 2030 figures given above, rather than the maturity values, govern the near-term assessment.

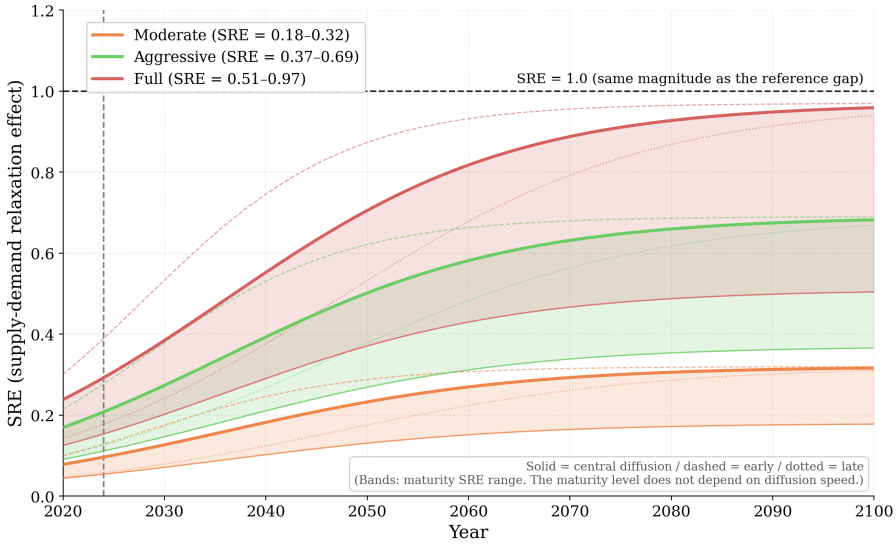


Figure 4. SRE trajectories: deployment scenario × diffusion scenario (2020–2100). Bands show the lower-to-upper range of the maturity SRE_{∞}; line styles show the diffusion scenario (solid = central, dashed = early, dotted = late). The SRE is a magnitude indicator that normalizes the relaxation capacity of AI by the 2030 reference gap (112 Mt), and SRE = 1 means only that the two are of the same magnitude; the effect on the actual year of self-sufficiency is shown in Figure 5. The vertical dashed line (2024) marks the last year of observed data and hence the boundary with the projection. G_{ref} = 112 Mt (112.26 Mt precisely; the 2030 baseline supply–demand gap under P2 × D-M × S-O) is the reference. The thick solid lines are the upper bounds under central diffusion, and the thin dashed and dotted lines are the corresponding upper bounds under early and late diffusion. The horizontal black dashed line marks SRE = 1.0, relaxation equal to the reference gap.

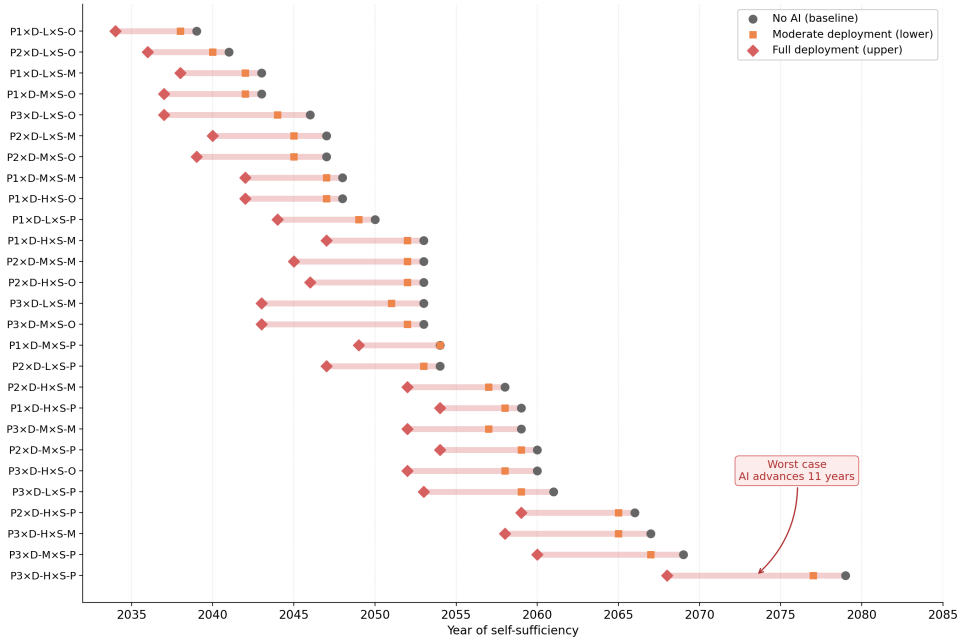


Figure 5. Year of self-sufficiency across the 27 scenarios and the advance brought about by AI (central diffusion). Grey circles: no AI (baseline); orange squares: moderate deployment; red diamonds: full deployment (upper bound of the effect). The length of each band is the number of years by which full deployment at its upper bound advances self-sufficiency (5–11 years; the moderate squares show the lower end of the effect). The later a scenario attains self-sufficiency, the longer the band—that is, the greater the marginal value of AI.

Table 9. Time series of SRE: deployment scenario × diffusion scenario (P2 × D-M × S-O baseline).

Deployment	Diffusion	2030	2050	2080	Maturity SRE_∞ ($A \to 1$)
Moderate	Early	0.10–0.18	0.17–0.29	0.18–0.32	**0.18–0.32**
	Central	**0.07–0.13**	**0.13–0.23**	**0.18–0.30**	**0.18–0.32**
	Late	0.05–0.08	0.10–0.17	0.16–0.29	**0.18–0.32**
Aggressive	Early	0.20–0.38	0.33–0.62	0.37–0.69	**0.37–0.69**
	Central	**0.15–0.27**	**0.27–0.50**	**0.35–0.66**	**0.37–0.69**
	Late	0.09–0.17	0.20–0.38	0.33–0.62	**0.37–0.69**
Full	Early	0.28–0.54	0.46–0.88	0.51–0.97	**0.51–0.97**
	Central	**0.20–0.39**	**0.37–0.71**	**0.49–0.93**	**0.51–0.97**
	Late	0.13–0.24	0.28–0.53	0.45–0.87	**0.51–0.97**

Note: Each value is computed as $SRE_t = SRE_\infty A(t)$. The deployment scenario sets the maturity effect size (the ceiling); the diffusion scenario sets the timing of its realization. Bold marks the reference case (central diffusion) and the maturity column. The rightmost column is the limit as $A \to 1$ and is therefore identical across diffusion scenarios. A common $A(t)$ is applied to all pathways.

We also verify whether the parameters adopted in our model (initial FCR value, loss rate, precision-agriculture adoption level) are consistent with observed data for 2000–2024. Table 10 compares the observed values and the model settings for the main parameters. All model initial values match the 2024 observations. The baseline scenarios on which this study builds have themselves been validated: Toyohara and Zhou [2] fitted the elasticity parameters of the food balance sheet to the observed C^* series for 2000–2024, drawn from NBS and U.S. Department of Agriculture (USDA) Production, Supply, and Distribution records, obtaining an annual mean error of +2.91%, a root mean square error of 5.35%, and an exact match at the 2024 validation point (projected C^* of 590 versus observed 590 kg/person/year). The parameters that this study adds to that baseline are validated separately in Table 10.

Table 10. Consistency of observed values and model settings for key parameters (2000–2024).

Parameter	Observed (∼2000)	Observed (∼2024)	Model Initial (2025)
Pig FCR (kg feed/kg meat)	≈4.0	≈3.0	3.0
On-farm storage loss rate (%)	≈8.0	≈3.0	3.0
Meat consumption (kg/p/yr)	≈53	≈75	75
C^* (kg/p/yr)	371	590	590
Agricultural drone cumulative operating area	pilot stage	2.67 bn mu-times (≈178 M ha)	early diffusion
Domestic production (Mt)	462	≈700	700

Data are based on NBS 2024, Toyohara and Zhou [2], Gaillard et al. [9] (FCR improvement mechanism), FAO [30] (feed and production), and the National Food and Strategic Reserves Administration (Grain Security Project; on-farm storage loss rate). The international reference level for losses (about 10% at the post-harvest handling and storage stage for cereals in industrialized Asia, a region that the source defines as Japan, China, and South Korea) is from Gustavsson et al. [17].

The above verification confirms that our model is consistent with the observed data for 2000–2024. In particular, the observed trajectory of FCR (4.0 → 3.0, a 25% improvement over 25 years) provides historical grounds supporting the technical feasibility of the additional improvement (3.0 → 2.5, a 17% reduction) that we assume through AI use. Likewise, the observed improvement in the loss rate (8.0% → 3.0%, a 62% reduction) has already been achieved through China's non-AI technology policy (the Grain Security Project), and the additional loss reduction through AI/IoT technology (3.0% → 1.5%) is therefore a

conservative assumption, amounting to only 30% of the improvement already achieved (1.5 of the 5 percentage points).

Finally, we classify the effect magnitudes of the five pathways into a demand side (improvement in grain use efficiency) and a supply side (additional production), organized in Table 11. Both contribute equivalently to mitigating the food supply–demand gap, but because their mechanisms differ, comparison is meaningful within each category.

Table 11. Representative effect magnitude of each pathway (2100 full technical potential; P2 × D-M × S-O basis).

Category	Pathway	Effect (Mt/Year)	Policy Priority
Demand side (grain use efficiency)	(1) Labor displacement → feed reduction	0.81–1.13	Low (secondary)
	(2) FCR improvement (precision livestock AI)	20.7–31.5	Highest (robust; requires public investment)
	(3) Industrial AI optimization	≈4	Medium (early realizable)
Supply side (production)	(4) Precision agriculture (S-O+ yield gain)	24–72	High (supply-side max)
	(5) Loss reduction	9.0–10.5	Medium-high (immediate)

Note: All magnitudes are the 2100 full technical potential (full AI deployment at maturity). The ranges are not all of one kind: the FCR row spans the population scenarios (its upper bound is the P3 value), row (1) spans the assumed meat reduction of 5–7 kg/person/year at P2, row (3) is a single P2 point, and the supply-side rows span the parameter uncertainty at P2. The demand side corresponds to improved grain use efficiency (how efficiently grain is used) and the supply side to increased production (how much is produced). Pathway (4) is the additional yield gain on the S-O trajectory from precision agriculture (ρ_{PA} = 2–6%; 1200 × ρ_{PA} Mt). Pathway (4b) (prevention of farmland abandonment) is conditional and is not counted here (Section 3.2).

As Table 11 shows, the largest effect on the demand side (grain use efficiency) is FCR improvement (Pathway (2), 20.7–31.5 Mt/year), substantially exceeding labor displacement (Pathway (1)). On the supply side, precision agriculture (Pathway (4)) has the largest effect magnitude, but this is additional production premised on realizing the S-O optimistic supply, differing in mechanism from demand-side FCR improvement. For the improvement in grain use efficiency that is the central concern of this study, the principal driver is FCR improvement, which supports placing this pathway at the top of the priority ranking for policy investment. Post-harvest loss reduction (Pathway (5)) has only a moderate effect magnitude but a high potential for immediate realization through "improvement of existing infrastructure", making it cost-effective as an early, short-term policy target.

3.5. Effect on the Year of Self-Sufficiency

Because China's population declines throughout this century, demand eventually falls below domestic production and self-sufficiency is attained with or without AI. The question is therefore not whether AI makes self-sufficiency possible, but when it brings about self-sufficiency, and by how much it thickens the surplus thereafter. Solving $G_t^{AI} \leq 0$ in Equation (2) for the 27 scenarios yields the year of self-sufficiency (Table 12, Figure 5).

Baseline self-sufficiency arrives in 2039 in the best scenario (P1 × D-L × S-O) and in 2079 in the worst (P3 × D-H × S-P), a span of 40 years. Full deployment of AI advances this by 2–11 years, but the effect differs sharply across scenarios. Under optimistic scenarios, self-sufficiency arrives in the late 2030s even without AI, so the advance is only 3–5 years. Under pessimistic scenarios, by contrast, self-sufficiency slips into the 2050s or 2070s and import dependence persists for decades; there AI advances self-sufficiency by up to 11 years and materially shortens the transitional period.

The same asymmetry appears in the surplus after self-sufficiency. In the reference scenario the 2100 surplus is a comfortable 841 Mt, and AI enlarges it by only 7–13%. In the worst scenario the surplus is a thin 265 Mt, and the AI effect (70–123 Mt under P3) enlarges it

by 26–47%. The marginal value of AI is thus greatest where the food balance is tightest: its relaxation capacity does its work not where the surplus is already thick, but where it is thin.

Table 12. Year of self-sufficiency and the advance brought about by AI (upper nine rows: D-M demand scenario; lower rows: the extremes of the 27 scenarios. Central diffusion throughout).

Scenario	No AI	Moderate	Full	Advance	Surplus Gain (2100)
P1×D-M×S-O	2043	2041–2042	2037–2040	3–6 yr	+5–11%
P1×D-M×S-M	2048	2046–2047	2042–2045	3–6 yr	+6–13%
P1×D-M×S-P	2054	2053–2054	2049–2052	2–5 yr	+8–17%
P2×D-M×S-O	**2047**	**2044–2045**	**2039–2043**	**4–8 yr**	**+7–13%**
P2×D-M×S-M	2053	2051–2052	2045–2050	3–8 yr	+8–16%
P2×D-M×S-P	2060	2058–2059	2054–2057	3–6 yr	+11–22%
P3×D-M×S-O	2053	2051–2052	2043–2048	5–10 yr	+11–19%
P3×D-M×S-M	2059	2056–2057	2052–2055	4–7 yr	+14–25%
P3×D-M×S-P	2069	2066–2067	2060–2064	5–9 yr	+22–39%
Best P1×D-L×S-O	2039	2037–2038	2034–2036	3–5 yr	+5–10%
Worst P3×D-H×S-P	**2079**	**2076–2077**	**2068–2073**	**6–11 yr**	**+26–47%**

Note: Bold marks the reference case (P2 × D-M × S-O) and the worst case. The year of self-sufficiency is the first year from which $G_t^{\mathrm{AI}} \leq 0$ holds permanently (the onset of a permanent surplus). The baseline trajectories of population, demand, and supply, and the definition of the year of self-sufficiency, follow Toyohara and Zhou [2]; the "No AI" column reproduces the published values of that study (earliest 2039, reference 2047, latest 2079). Diffusion is central ($k = 0.070$, $t_0 = 2036$). The range of years corresponds to the lower and upper bounds of the effect magnitude. Because the demand-side effects of AI scale with population, $\Delta S_\infty^{\mathrm{AI}} + \Delta D_\infty^{\mathrm{AI}}$ under full deployment is 50–101 Mt for P1, 57–109 Mt for P2, and 70–123 Mt for P3.

3.6. Sensitivity Analysis

The SRE value is sensitive to several parameters. Here we present the sensitivity to six items: the FCR improvement magnitude, the reference gap G_{ref} (supply scenario and reference year), the two secondary pathway parameters, the precision-agriculture effect, the social safety-net coefficient, and the AI diffusion speed.

The FCR improvement magnitude ($\Delta\varphi = \varphi_0 - \varphi_{\mathrm{AI}}$) is the largest contributing factor in the numerator of the SRE. We estimate the FCR effect magnitude and its impact on full-deployment SRE when $\Delta\varphi$ varies from the baseline value of 0.5 (Table 13). A change in $\Delta\varphi$ leaves the effect magnitudes of the other four pathways (labor displacement, industrial AI, precision agriculture, loss reduction) unchanged. The SRE therefore does not shrink in proportion to $\Delta\varphi$; it falls only by the loss on the FCR pathway. Even at the most conservative post-AI FCR = 2.8 ($\Delta\varphi = 0.2$), the SRE is 0.13–0.26 under moderate deployment and 0.40–0.86 under full deployment, exceeding the labor-displacement effect (0.001–0.010) by one to two orders of magnitude. The conclusion of this study—that the primary channel of AI's contribution is FCR improvement rather than labor displacement—therefore holds even under the most pessimistic estimate of the FCR gain. At the upper bound of full deployment, by contrast, the SRE reaches only 0.97 at the reference $\Delta\varphi = 0.5$ and stays at or below 0.94 for $\Delta\varphi \leq 0.4$. The relaxation capacity of full deployment therefore remains below the 2030 reference gap across this range; this is a statement about magnitude, not about whether the gap is eventually closed, which population decline settles in every scenario (Section 3.5).

We next examine the sensitivity of the SRE to the choice of the reference gap itself, in two directions: the supply scenario on which G_{ref} is evaluated, and the reference year (Table 14). Because the numerator (the pathway effects) is unaffected, changing the denominator rescales all SRE values by a common factor and leaves the ranking of the pathways, and every conclusion drawn from it, unchanged. Evaluating G_{ref} under the medium supply scenario S-M (148.3 Mt) or the pessimistic scenario S-P (188.3 Mt) instead of the optimistic S-O lowers the full-deployment maturity range from 0.51–0.97 to 0.38–0.74 and 0.30–0.58, respectively. S-O is retained as the reference because it is the supply assumption of the baseline case itself, so that the numerator and the denominator remain internally consistent. Shifting

the reference year has a stronger effect on the denominator: in 2025 the interpolated gap is 123.1 Mt (full deployment 0.46–0.89), while by 2040 population decline has shrunk the baseline gap to 53.6 Mt, so the same effects amount to 1.06–2.04 times the gap. This is the divergence problem that motivates a fixed reference (Section 2.1): as the baseline approaches self-sufficiency the denominator vanishes. We adopt 2030 because it lies at the center of the transitional decade in which the baseline import dependence is heaviest (12–14%), is the nearest decadal year for which the baseline of Toyohara and Zhou [2] reports all three axes, and precedes the baseline year of self-sufficiency (2047) by a wide margin.

Table 13. Sensitivity to the FCR improvement magnitude (P2 × D-M × S-O, at maturity).

$\Delta\varphi$ †	Post-AI FCR†	FCR Effect	SRE_∞		
		(Mt/Year)	Moderate	Aggressive	Full
0.2 (conservative)	2.8	8.28	0.13–0.26	0.28–0.60	0.40–0.86
0.3	2.7	12.42	0.15–0.28	0.31–0.63	0.43–0.90
0.4	2.6	16.56	0.17–0.30	0.34–0.66	0.47–0.94
0.5 (reference)	2.5	20.70	0.18–0.32	0.37–0.69	0.51–0.97

Note: † Both $\Delta\varphi$ and the post-AI FCR are the values attained at full deployment (100% uptake); under moderate and aggressive deployment, 50% and 80% of the gain are realized, respectively (Table 8). Because a change in $\Delta\varphi$ leaves the other four pathways unchanged, the SRE is computed by subtracting only the loss on the FCR pathway.

Table 14. Sensitivity of the maturity SRE_∞ to the reference gap: supply scenario and reference year.

Reference Basis	G_{ref} (Mt)	Moderate	Aggressive	Full
2030, S-O (reference)	**112.26**	**0.18–0.32**	**0.37–0.69**	**0.51–0.97**
2030, S-M	148.3	0.14–0.24	0.28–0.52	0.38–0.74
2030, S-P	188.3	0.11–0.19	0.22–0.41	0.30–0.58
2025, S-O	123.1	0.17–0.29	0.34–0.63	0.46–0.89
2040, S-O	53.6	0.38–0.67	0.77–1.44	1.06–2.04

Note: Bold marks the reference basis used in the main analysis. The numerator (pathway effects at maturity) is identical across rows; only the denominator changes, so all values in a given row differ from those in the reference row by a common factor and the pathway ranking is invariant. The 2025 and 2040 gaps are linear interpolations of the model trajectory that underlies Table 3 (P2 × D-M × S-O), the same trajectory used for the year of self-sufficiency in Section 3.5. The population keypoint of that trajectory at 2020 is the model value of the baseline study (1426 million), which differs slightly from the observed 1412 million shown in Table 3; recomputing the 2025 gap from the printed 2020 column therefore gives a slightly smaller value. The 2040 row illustrates the divergence that motivates a fixed reference gap: as the baseline approaches self-sufficiency (2047), the denominator shrinks and the ratio inflates without any change in the underlying AI effect.

The two remaining pathway parameters not yet varied, the industrial-AI efficiency gain η_{ind} and the AI loss-rate reduction, are examined in Table 15. Both enter the SRE linearly, and their entire plausible ranges move the maturity SRE_∞ by only about 0.02 and 0.06, respectively—an order of magnitude below the contribution of the FCR pathway (0.18 in SRE units) in the first case and about a third of it in the second, and far below that of precision agriculture (0.21–0.64) in both. Neither parameter can therefore alter the ranking of the pathways or any conclusion of this study; their uncertainty is absorbed within the deployment-scenario ranges already reported.

The impact of variation in the precision-agriculture effect (ρ_{PA}) on the S-O+ scenario supply volume and on the worst-case surplus is shown in Table 16. A ± 0.02 variation in ρ_{PA} shifts the surplus by about 24 Mt, of the same order of magnitude as the FCR improvement effect (a demand reduction equivalent to about 21 Mt/year). The uncertainty in the precision-agriculture effect therefore does not change the direction of the conclusions.

Table 15. Sensitivity to the secondary pathway parameters η_{ind} and the loss-rate reduction (P2 × D-M × S-O, maturity, full deployment).

Parameter	Low/Central/High	Effect (Mt/Year)	SRE_∞ Contribution
η_{ind} (industrial AI)	0.05/0.08/0.10	2.5/4.0/5.0	0.022/0.036/0.045
Loss-rate reduction (pp) ‡	0.5/1.0/1.5	3.5/7.0/10.5	0.031/0.062/0.094

Note: ‡ pp = percentage points. Effects are computed from Equation (9) ($P \times C^*_{\text{ind}} \times \eta_{\text{ind}}$, P2 2100 basis) and from the loss identity (production ≈ 700 Mt × reduction in the loss rate); contributions are obtained by dividing by G_{ref} = 112.26 Mt. For comparison, the FCR pathway contributes 0.18 and precision agriculture 0.21–0.64 in the same units. The ranges are the full plausible spans set in Section 2.2 and Table 4: η_{ind} = 0.05–0.10 extends mechanistic evidence from fermentation optimization, and the loss-rate reduction of at most 1.5 points equals only 30% of the 5-point improvement already delivered by the non-AI Grain Security Project, so the upper bounds are themselves conservative.

Table 16. Sensitivity to the precision-agriculture yield gain (2100 supply, P2 × D-M surplus and P3 × D-H × S-P surplus).

ρ_{PA} (Precision-ag Effect)	S-O+ Supply	P2×D-M Surplus (S-O+)	P3×D-H×S-P Surplus
0.02 (lower)	1224 Mt	865 Mt	282 Mt
0.04 (median)	1248 Mt	889 Mt	299 Mt
0.06 (upper)	1272 Mt	913 Mt	317 Mt

Note: The worst-case column (P3 × D-H × S-P) applies the ρ_{PA} yield gain to the supply volume of the S-P trajectory, so the multiplicand differs from the S-O baseline of Equation (11).

The social safety-net coefficient γ is a threshold-type parameter that determines whether the "demand contraction" from labor displacement translates into improved food security or into nutritional deficiency. For $\gamma = 0.8$, the income of displaced workers is largely maintained, and the consumption reduction remains small (SRE contribution 0.003–0.004). For $\gamma < 0.4$, the risk of post-displacement consumption collapse increases, and the pathway may become counterproductive as a food-security policy. This pathway must be examined in conjunction with economic distribution policy, and it should be treated as a risk-management issue separate from FCR improvement, the primary demand-side driver of SRE.

Finally, we examine the uncertainty about the timing of AI diffusion. Because the diffusion speed cannot be calibrated from data, we represent it by three scenarios: early, central, and late (Table 2). As Table 9 shows, the diffusion scenario moves the SRE in any given year substantially: the 2030 SRE under full deployment is 0.13–0.24 under late diffusion but 0.28–0.54 under early diffusion. Even at the upper bound of full deployment, however, the SRE in 2100 is 0.97 under early diffusion, 0.96 under central diffusion, and 0.94 under late diffusion, so the difference across diffusion scenarios is small. The maturity value SRE_∞ ($A \to 1$), moreover, is identical across all three diffusion scenarios—0.18–0.32, 0.37–0.69, and 0.51–0.97. What diffusion uncertainty governs is when the relaxation is attained, not how much relaxation is attainable. For the former, the scenario range above delimits the span.

We also examined the heterogeneity of diffusion speed across pathways. The five pathways do not in fact diffuse at the same rate: precision agriculture (drone-based application and the like) can be procured as an outsourced service at low capital cost, and therefore spreads rapidly, whereas genomic breeding, the core of FCR improvement, is rate-limited by generation turnover and advances only slowly. We applied a common $A(t)$ to all pathways for the sake of parsimony, and confirmed by a bounding check that this simplification does not distort the conclusions. Classifying the pathways by technological characteristics into fast (precision agriculture, loss reduction), medium (labor displacement, industrial AI), and slow (FCR improvement), and recomputing $\text{SRE}_t = \sum_i \Delta E_i A_i(t)/|G_{\text{ref}}|$ with pathway-specific diffusion curves, leaves the maturity SRE_∞ entirely unchanged and shifts

the 2030 SRE by no more than 0.06 (pathway-specific curves: fast $k = 0.15$, $t_0 = 2030$–2032; medium $k = 0.10$, $t_0 = 2036$; slow $k = 0.06$, $t_0 = 2042$). The two estimates diverge most in mid-century (2040–2050, by at most 0.17), where the common-$A(t)$ estimate is the more conservative, because precision agriculture, the pathway with the largest effect, is also the fastest to diffuse. The bias of the simplification is therefore bounded and signed: it leaves SRE_∞ exactly unchanged and errs on the conservative side throughout the transition.

We further examine the consequences of each deployment scenario being a composite of five pathways. The drivers of the five pathways are mutually independent, and it is entirely possible for market-led precision agriculture to diffuse rapidly while FCR improvement, which depends on public research and development, is left behind. Because the SRE is defined as the additive sum of the pathway effects (Equation (3)), however, whatever levels the five pathways independently take, SRE_∞ necessarily lies within the interval bounded by the case in which all pathways sit at the lower bound of moderate deployment and the case in which all sit at the upper bound of full deployment. That interval is 0.18–0.97, and its endpoints coincide with those of the three deployment scenarios (the lower bound of moderate, 0.18, and the upper bound of full, 0.97). The assumption that the pathways move together therefore does not alter the interval within which SRE_∞ can fall; the three deployment scenarios are to be read as representative points within it. What decoupling does govern is which point within the interval is realized. An asymmetric decoupling—in which market-driven precision agriculture runs ahead while FCR improvement, dependent on public research and development (R&D), lags—is particularly likely, and the prioritization in Section 4.4 is aimed precisely at correcting that asymmetry.

4. Discussion

4.1. Risk Assessment

The expansion of AI agriculture entails several side effects, ranging from energy load to policy risk, and we examine four principal categories in turn.

The most direct concern is the energy and climate cost. AI robot operation under the aggressive deployment scenario would add 30–60 TWh/year of additional electricity demand. Unless China's power mix shifts toward renewable energy, the resulting increase in CO_2 emissions could accelerate, through climate change, the shift toward the S-M/S-P trajectories. A scenario in which the supply-strengthening effect of AI agriculture is offset by worsening climate impacts cannot be excluded.

A second concern is unemployment and inequality. When the social safety net for displaced workers is inadequate ($\gamma \to 0$), the income loss accompanying the decline in activity levels manifests as consumption collapse. In that case, the benefit of demand reduction appears as nutritional deficiency rather than as improved food security. The SRE of this analysis is sensitive to the sufficiency of the social safety net (γ), and adequate income-compensation policy during the transition period is indispensable.

Diffusion lag is a third concern. FCR improvement (precision feeding, genomic breeding) and precision-agriculture AI each face an expected time lag of 10–20 years before substantial diffusion into Chinese agriculture. If diffusion to small- and medium-scale farms (over 70% of all farms) is delayed, the effect magnitudes assumed in these estimates will be overestimates.

A fourth concern is data security and policy risk. AI agricultural infrastructure entails centralized management of crop data, producer information, and logistics data, and the balance between state data control and private use may become problematic. In particular, bridging the regional divide in precision agriculture requires public investment in digital infrastructure and rural support measures.

4.2. Positioning Relative to Prior Research

This study isolates the contribution of AI technologies to China's food supply–demand balance from that of the baseline. Table 17 presents a comparison with prior research.

Table 17. Comparison with prior research.

Study	Focus	Key Finding	Relation to This Study
Wolfert et al. [7]	Agricultural big data	Data use extends to the redesign of the entire supply chain; the discussion centers on governance and business models	Does not quantify food demand or grain use efficiency
Halachmi et al. [8]	Precision livestock sensors	Real-time sensors improve livestock health and productivity	Technical basis for Pathway (2); this study connects FCR improvement to a food supply–demand model
Lopez et al. [10]	Pig genomic selection	Raises the annual monetary genetic gain by 9–12%, and the annual gain in FCR alone by 7–15%	Direct evidence for Pathway (2) (breeding effect)
Getahun et al. [5]	Precision-agriculture technologies	Gains in yield and resource efficiency (systematic review)	Evidence for Pathway (4); applied conservatively (2–6%) in the S-O+ scenario
Sheng et al. [31]	China agricultural total factor productivity (TFP)	TFP growth and drivers (1978–2016)	AI and demand-side effects not analyzed
Toyohara & Zhou [2]	China food supply and demand	Surplus in all 27 scenarios by 2100; import dependence 12–14% (2030)	Baseline of this study; the AI effect (self-sufficiency advanced by 2–11 years; the 2100 surplus enlarged by 5–47%) is layered on top
This study	AI × food supply and demand	Quantifies five SRE pathways; self-sufficiency advanced by 2–11 years and the 2100 surplus enlarged by 5–47%, the effect growing with the severity of the scenario	First presentation of the SRE framework; positions AI as insurance against adverse futures

The prior studies in Table 17 fall into two groups. The first establishes the technical foundations of individual pathways: precision-livestock sensing and breeding underlying Pathway (2), and precision-agriculture technologies underlying Pathway (4) [5,8,10], with Wolfert et al. [7] addressing the governance and business-model conditions for data use across the supply chain. The second comprises productivity analyses that do not treat AI or demand-side effects [31]. None connects these mechanisms to a long-term food supply–demand model. Building on the 27-scenario baseline of Toyohara and Zhou [2] (a surplus in all scenarios by 2100; 2030 import dependence 12–14%), the present study quantifies the five SRE pathways and identifies FCR improvement (20.7 Mt/year) as the primary driver of grain-use-efficiency improvement, presenting the SRE framework for the first time.

The positioning of this study relative to prior research can be organized as follows. The SRE analysis first shows that even the moderate scenario delivers, at maturity, a relaxation capacity equal to 18–32% of the 2030 reference gap (112 Mt). Even under conservative assumptions that exclude any AI effect, a food surplus is confirmed in all scenarios by 2100 [2]. The additional effect of AI deployment estimated here widens that margin, and the medium-term (2030) import dependence of 12–14% shown by the same study

could be reduced to 10–13% through the 0.9–1.6 percentage-point reduction delivered by moderate deployment (diffusion is still under way in 2030, so the reduction is smaller than at maturity), which is also consistent with the Chinese government's food self-sufficiency target (≥95% for grains). Finally, the worst-case (P3 × D-H × S-P) surplus of 265 Mt expands to 299 Mt when the precision-agriculture gain is applied to the S-P supply volume, raising it from 860 to 894 Mt, and combining full SRE deployment increases it further. In short, the SRE analysis of this study shows that, even under pessimistic climate and population conditions, the deployment of AI technology adds to the margin of food security.

Although our framework targets China, comparison with other major countries clarifies its implications. Under the Common Agricultural Policy (CAP), the EU promotes precision agriculture and digitalization in a subsidy-led manner: all 27 Member States set out a digitalization strategy in their 2023–2027 CAP Strategic Plans, albeit of varying depth, and seven of the 28 plans (Belgium submits two) intend to establish a dedicated eco-scheme compensating farmers for the use of precision-farming technologies [32]. AI-driven resource-efficiency improvement is tied to regulatory compliance: against the backdrop of the Nitrates Directive [33], the Farm to Fork strategy targets a reduction of nutrient losses by at least 50%, which the Commission expects to reduce fertilizer use by at least 20% by 2030, positioning precision fertilization as a means to that end [34]. Backed by large-scale mechanized agriculture, the United States shows high adoption rates of precision agriculture. Guidance systems covered 58% of planted corn acres in 2016, and auto-steer alone reached 72.9% of sorghum and 64.5% of cotton acres in 2019 (the survey definition narrows to auto-steer only from 2018, so the two figures are not strictly on the same basis), whereas variable-rate technology (VRT) remained at 37.4% of corn-planted acres in 2016 and 25.3% of soybean-planted acres in 2018 [35]. The motivation for adoption lies in both labor saving and the optimization of inputs (fertilizer, fuel), and considerable room for input optimization remains [35,36]. Adoption on non-mechanized farms is almost nonexistent [36], largely because few precision-agriculture technologies have been developed or commercialized for such farms. In Japan, the aging of the agricultural workforce and the shortage of successors are acute: core agricultural workers fell to 1.114 million in 2024 (mean age 69.2 years; 71.7% aged 65 or over), and abandoned farmland reached 257,000 ha as of March 2024 [37]. The primary motivation for adopting AI and robots is to offset the labor shortage; the government holds that "accelerating productivity growth by promoting the use of smart agricultural technology is indispensable for sustained food supply" and enacted the Act on Promotion of Smart Agricultural Technology in 2024 [38]. This concern is closely related to the prevention of farmland abandonment that this study discusses qualitatively as a conditional supply-side effect (pathway (4b), the S-P → S-O trajectory shift). China, by contrast, is distinctive in that the effect of FCR improvement (demand side) is exceptionally large, reflecting the world's largest livestock sector (pork production), and this study's finding that "the primary channel of grain-use-efficiency improvement is FCR" carries implications specific to a major livestock producer. The SRE framework itself is dimensionless, and re-evaluating the pathway-specific contributions in line with each country's technological and industrial structure would allow it to be generalized as an internationally comparable policy-evaluation metric.

4.3. Model Limitations and Future Work

The analysis has several limitations, beginning with the static nature of the model and the abstraction from regional heterogeneity.

The first limitation is the absence of a dynamic model. The five-pathway quantification of this study is primarily a static, scenario-based assessment centered on the "endpoint level" around 2100. A dynamic model that internalizes AI diffusion cost, diffusion speed,

and interactions (e.g., the complementary effect of precision agriculture and genomic breeding) is a future task. A concrete route is to attach to each pathway a cost function and an adoption-decision rule (capital outlay, operating cost, and payback period at farm or firm level), embed the five pathways in a dynamic investment-optimization model, and solve for the deployment path endogenously instead of imposing deployment scenarios; the cost estimates required for the investment ranking of Section 4.4 would emerge from the same exercise.

The second limitation is the abstraction from regional heterogeneity. Within China, large gaps in AI diffusion speed exist between coastal, large-scale farms and inland, small-scale farms. The national-average FCR and loss rates of this study abstract from regional heterogeneity, and may overestimate "nationwide diffusion." Provincial panel data on machinery investment, drone-service coverage, and livestock-farm scale would permit estimating the diffusion curve $A(t)$ separately for coastal and inland provinces, replacing the single national logistic with a two-tier specification.

The demand-side model is also simplified. The food balance sheet approach (aggregated C^*) cannot capture commodity-specific structural changes in meat, soybeans, cereals, and the like. Since the effect of FCR improvement differs by species and commodity, verification using a commodity-disaggregated model is warranted. A tractable next step is a five-commodity balance (rice, wheat, maize, soybeans, and others) with an explicit soybean-meal inclusion-rate parameter, which would connect the FCR pathway directly to the soybean import question raised below.

A related limitation is that the five pathways are tied to a single deployment scenario, so the possibility that they move independently is not modeled explicitly. By the additivity of the SRE, independent movement leaves the attainable interval unchanged (Section 3.6), but which point within the interval is realized depends on how the pathways decouple; a formulation that treats pathway-level realization rates independently remains for future work.

The interaction with climate change is likewise not fully treated. The SRE analysis takes the supply scenarios (S-O/S-M/S-P) of Toyohara and Zhou [2] as given, but the risk that AI-technology diffusion increases electricity consumption and exerts pressure toward S-P is noted only in the risk assessment (Section 4.1). A more precise coupled climate–technology model is a research task to be combined with the simplified demand-side model above.

Parameter validation also has its limits. The FCR improvement magnitude ($\Delta\varphi = 0.5$) is estimated from the findings of existing literature, but empirical data at commercial scale in China are limited. In particular, the empirical effect of genomic breeding 10–20 years hence cannot be observed at the time of writing. The adoption rate $A(t)$ carries a further limitation: as noted in Section 2.1, it cannot be calibrated from any existing statistic. We therefore treat $A(t)$ as a diffusion scenario rather than an estimate, and attach a range through the early, central, and late cases (Table 2). The premise that $A(t) \to 1$, that is, that the chosen deployment scenario is fully realized by 2100, nonetheless remains untested. Should penetration among small-scale farms stall permanently, the effect realized would fall below what each deployment scenario assumes. Uncertainty about this ceiling is carried by the range spanned by the moderate, aggressive, and full deployment scenarios.

Social and political feasibility lies outside our scope as well. Realizing full SRE deployment (SRE = 0.51–0.97) requires large-scale public support for farm operators, agricultural digital-transformation policy, and rural digital-infrastructure development. The feasibility of satisfying these policy conditions falls within the domain of agricultural policy research and lies outside the scope of this study.

The treatment of soybean and feed commodities remains a further task. Most of China's import dependence (approximately two-thirds of gross grain imports by volume) consists of soybeans, but the C^* of this study is an aggregate grain-equivalent indicator.

Research that disaggregates the improvement in soybean self-sufficiency by commodity may have more directly relevant implications for food-security policy.

A related limitation concerns the scope of the food-security concept. As stated in Section 2.1, this study addresses only the availability dimension among the four, that is, the aggregate grain-equivalent balance; affordability, nutritional quality and utilization, and the stability of access under shocks are not modeled. A national aggregate surplus can therefore coexist with insecurity for particular households, regions, or commodities, and the conclusions of this study should be read as statements about aggregate availability. Coupling the SRE to prices, income distribution, and reserve policy so as to reach these dimensions remains a task for future research.

Finally, the scope of the labor-displacement effect is limited. We evaluated the impact of AI-driven labor displacement on food supply and demand only as the "marginal contraction of consumption accompanying lower activity levels." We showed that this effect is small and that the primary channel of AI's contribution to food security is FCR improvement (grain use efficiency); this does not, however, mean that AI-driven labor displacement itself is small. Econometric analysis of economy-wide, all-industry labor displacement by AI and its spillovers to income, employment, and food consumption is beyond the scope of this study and will be reported in a follow-up paper.

4.4. Policy Implications

From the above assessment, five policy directions follow: demand rationalization, precision livestock farming, worker protection, bridging the regional divide, and linking population policy to AI investment.

As a way of putting the SRE to work in these strategies, the following policy cycle can be envisioned. The cycle begins by using the SRE to quantify the relaxation capacity of each pathway, so that the contribution of limited AI investment to closing the supply–demand gap can be assessed on a common scale. Investment priorities then follow from that quantification: our estimates indicate that FCR improvement has the largest relaxation capacity on the demand side (grain use efficiency) and precision agriculture the largest on the supply side, so these two pathways rank highest in the allocation of investment. Once investment has been made, the SRE actually realized is verified against the observed reduction in import dependence, which links the framework to policy evaluation, and the results of that evaluation are converted into cost-effectiveness per unit of SRE to serve as the basis for budget allocation. This study, however, does not treat the adoption cost of each pathway, and the cost estimates required for this conversion remain a task for future work. The cycle closes by incorporating the SRE into the national food-security strategy as one of its key performance indicators and feeding it back into the next investment plan. Repeating this cycle allows AI investment to be revised on quantitative grounds.

The policy-engineering value of the SRE rests on its being a dimensionless common scale. Whereas the self-sufficiency ratio and the import dependency ratio merely describe the outcome of supply and demand, the SRE measures how far an intervention can move that outcome. AI technologies whose technical mechanisms differ (precision livestock farming, precision agriculture, industrial AI, and loss reduction) can therefore be compared and ranked within a single framework.

Demand rationalization should be set as a national target. The D-L scenario of Toyohara and Zhou [2] (C^{*}_{2100} = 650 kg/person/year, East Asian saturation type) corresponds to a level approximately 17% below the current trajectory (D-M: 780 kg/person/year) in 2100. Combining food-education and food-culture policy (e.g., the "Clean Plate Campaign" against food waste) with AI supply optimization could induce this trajectory shift. If a shift to D-L is achieved by 2050, this would amount to a demand reduction of approximately

70 Mt/year under the P2 scenario, and combined with the SRE effect, it is estimated to advance the elimination of import dependence by about 10 years.

Priority in deployment should go to precision livestock AI. The grounds for this, however, do not lie in a simple comparison of effect magnitudes. Judged purely on magnitude, the yield gain from precision agriculture (Pathway (4), 24–72 Mt/year) exceeds that from FCR improvement (Pathway (2), 20.7–31.5 Mt/year). We nevertheless place FCR improvement at the top of the public-investment ranking, for three reasons. First, the effect of precision agriculture is a conditional upside premised on realizing the optimistic S-O supply trajectory, whereas FCR improvement is a robust effect that materializes in all 27 scenarios irrespective of the supply trajectory. Second, drone-based application—the core of precision agriculture—can be procured as an outsourced service at a low capital barrier and is already diffusing rapidly under market forces, so the scope for public investment to accelerate it further is comparatively small. Third, genomic breeding, which is central to FCR improvement, is a cumulative process rate-limited by generation turnover. The generation interval in pigs is about 1.7–1.9 years, genomic selection shortens it by only about 10%, and raising breeding investment by 35–89% increases the annual genetic gain by only around 10%—in some configurations lowering profit [10]. The rate of genetic gain is not something that capital input can compress. We assume that a substantive improvement in FCR requires the accumulation of several generations, on the order of 10–20 years; this is precisely the horizon that private investment decisions are least likely to reach, so progress depends on long-horizon public research and development. In short, public resources should be concentrated on pathways that markets are unlikely to deliver and that do not depend on favorable supply conditions, and by this criterion FCR improvement ranks highest. As the sensitivity analysis (Table 13) shows, even the conservative $\Delta\varphi = 0.3$ secures a reduction of 12.42 Mt/year. Concrete policy instruments include purchase subsidies for precision feeding systems (IoT/AI automated control) allocated with priority to small- and medium-scale farms, the national development of AI-accelerated genomic breeding centers with R&D subsidies for breeding enterprises, and the construction of AI-based early disease-monitoring networks for swine fever and other diseases through coordination between the Ministry of Agriculture and Rural Affairs and local governments. The 20.7 Mt of feed-grain saving in these estimates is the value obtained by multiplying the 2100 P2 total meat consumption (460 million $\times$ 90 kg = 41.4 Mt) by an FCR improvement of 0.5 units (for reference, China's 2024 pork production was approximately 57 Mt).

The third direction is to establish social safety nets for workers during the transition. As the sensitivity analysis shows, at a social safety-net coefficient $\gamma < 0.4$, labor displacement carries the risk of consumption collapse. A target of $\gamma \geq 0.9$ should be set, and income compensation and job-transition training for AI-displaced workers should be institutionalized. China's rural surplus labor (estimated at over 100 million people) and urban unskilled workers (estimated at 200 million) are segments with high transition risk, and it is difficult to realize the policy benefits of SRE without support for these groups. Although the effect of γ variation on aggregate SRE is small in these estimates (a contribution of 0.001–0.010 across the deployment scenarios), the impact on the standard of living of individual workers is severe, and this response is indispensable from the standpoint of social equity.

The fourth direction is to bridge the regional divide in AI agricultural infrastructure. One of the greatest challenges for Chinese agriculture is the digital divide affecting rural areas and small-scale farms. Over 70% of agricultural operations are small-scale farms (operating area under 2 ha), and realizing the S-O+ scenario is difficult without AI diffusion to them. The diffusion of precision-agriculture AI (which realizes the S-O+ scenario) requires several public investments as preconditions: the development of rural broadband

and 5G by accelerating the Ministry of Agriculture and Rural Affairs' "Digital Village" plan, the establishment of an AI agricultural advisory system for farmers through the digitalization of agricultural extension officers, and agricultural digital-transformation subsidies for small-scale farms together with public support for drone pesticide-spraying services. Realizing $\rho_{PA} = 0.04$ (median) is estimated to require diffusion to over 50% of the national area, but because the current diffusion rate is biased toward intensive, large-scale farms, only about half of the upper-bound effect can be expected without bridging the regional divide.

The fifth direction, which ties the others together, is to link population policy to AI investment. As Section 3.5 shows, the marginal value of AI is greatest in scenarios in which the food balance is tightest. If policy aims to recover fertility and sets a high population target (P3, 700 million in this study), self-sufficiency slips to 2079 in the worst scenario and import dependence persists for nearly half a century. On that trajectory AI advances self-sufficiency by 6–11 years and enlarges the thin 2100 surplus (265 Mt) by 26–47%. Under a low-population trajectory (P1, 320 million) with favorable demand, by contrast, self-sufficiency arrives as early as the late 2030s even without AI, and the contribution of AI is limited. In other words, the higher the population target a policy sets, the closer AI investment comes to a necessary condition rather than an option. Population policy and AI agricultural investment cannot be decided independently; they should be designed as a single policy package.

5. Conclusions

This paper formulated the impact of AI robot technology on China's food supply–demand balance as the "Supply–Demand Relaxation Effect (SRE)" and analyzed it through a decomposition into five pathways.

The findings can be organized in academic, methodological, and policy terms.

Academically, we showed that the introduction of AI robots produces a dual effect, "supply augmentation" (precision agriculture, loss reduction) and "demand rationalization" (FCR improvement, industrial AI), and made clear that the conventional implicit premise that "AI strengthens supply but does not affect demand" is incomplete. In particular, the finding that the primary channel of AI-driven grain-use-efficiency improvement is not labor displacement but FCR improvement shifts the understanding of the food-security effect of AI agriculture away from the conventional labor-displacement-centered view.

Methodologically, we proposed the indicator "SRE", which measures the marginal improvement capacity of a specific intervention (AI adoption) as a dimensionless quantity. The SRE quantifies the "mitigation contribution of a technology" that existing indicators describing the state or outcome of supply and demand (self-sufficiency ratio, import dependency, supply gap) cannot measure, and enables heterogeneous AI technologies to be compared and ranked on a common scale (Table 1). We then decomposed the SRE into five pathways and formalized the effect magnitude of each pathway and how it emerges over time through the AI adoption rate $A(t)$.

In policy terms, we showed that the value of AI grows with the severity of the scenario. China's population decline means that self-sufficiency will eventually be attained, but the date at which it arrives spans a 40-year range in the baseline, from 2039 to 2079. AI advances this by 2–11 years and enlarges the post-self-sufficiency surplus by 5–47%. Both effects are larger the higher the population, the higher the demand, and the more pessimistic the supply. AI is not a means of adding to the surplus in futures that go well; it is insurance against futures that do not. The higher the population target a policy sets, therefore, the closer AI agricultural investment comes to being a necessary condition, and the two should be designed as a single package. In allocating investment, precision agriculture has the larger effect magnitude, but FCR improvement (precision livestock AI) should rank highest,

being independent of the supply scenario and unlikely to be delivered by the market. This ranking rests on relaxation capacity and on the likelihood of market under-provision, not on a full cost-effectiveness comparison: pathway-level adoption costs are not estimated in this study, and the ranking should be revisited once such estimates become available (Section 4.3). The surplus is a grain-equivalent aggregate and does not by itself guarantee commodity-level security. For the transitional period (import dependence of 12–14% on a 2030 basis), the reduction is limited to 0.9–1.6 percentage points under moderate deployment and to 2.6–5.0 points even under full deployment: because diffusion is still under way, the contribution of AI at that date is modest.

In our assessment, the significance of these results lies less in the magnitude of the relaxation that AI can deliver than in when, and under what conditions, it matters. China attains grain self-sufficiency in the aggregate under every scenario we examine, so the case for investing in agricultural AI cannot rest on averting an aggregate shortfall. What it can rest on is narrower. The value of AI is concentrated in the futures that go badly, which places it closer to insurance than to a growth strategy, and this is also why we rank FCR improvement above precision agriculture despite its delivering the smaller effect of the two: the binding constraint there is generation turnover in genomic breeding, which capital input cannot compress and which the market is therefore least likely to relieve on its own. It is equally worth stressing what an aggregate surplus does not settle. What we report is an aggregate, and the commodity composition behind it, soybeans above all, remains an open problem that this framework does not resolve. We caution, then, against reading these results as an argument that technology removes the need for demographic or trade policy; they suggest rather that AI investment, population policy, and trade policy have to be designed together.

As for future research, the construction of a dynamic model that endogenizes regional disparities in AI diffusion speed and the interaction effects with energy transition and climate change is needed. In addition, econometric analysis addressing economy-wide, all-industry spillovers to labor, employment, and income of the AI-driven labor displacement that this study evaluated only as "lower activity levels" will be reported in a follow-up paper.

Author Contributions: Conceptualization, A.T. and W.Z.; methodology, A.T.; validation, A.T. and W.Z.; formal analysis, A.T.; investigation, A.T.; data curation, A.T.; writing—original draft preparation, A.T.; writing—review and editing, A.T. and W.Z.; visualization, A.T.; supervision, W.Z. All authors have read and agreed to the published version of the manuscript.

Funding: This research received no external funding.

Institutional Review Board Statement: Not applicable.

Informed Consent Statement: Not applicable.

Data Availability Statement: The study uses only publicly available data from the National Bureau of Statistics of China (NBS), FAO, and FAOSTAT, together with the published baseline scenarios of Toyohara and Zhou (2026), *Sci* 8(7), 151 (https://doi.org/10.3390/sci8070151) [2]. The analysis scripts and derived results that reproduce all reported values, tables, and figures are available from the corresponding author on reasonable request.

Acknowledgments: The authors thank colleagues at the Graduate School of Policy Science, Ritsumeikan University, for the helpful discussions on the supply–demand relaxation effect framework.

Conflicts of Interest: The authors declare no conflicts of interest.

References

1. United Nations, Department of Economic and Social Affairs, Population Division. World Population Prospects 2024: Summary of Results (UN DESA/POP/2024/TR/NO. 9). 2024. Available online: https://population.un.org/wpp/assets/Files/WPP2024_Summary-of-Results.pdf (accessed on 16 August 2026).
2. Toyohara, A.; Zhou, W. Can China feed itself by 2100? Long-term food security under population decline: An integrated 27-scenario analysis. *Sci* **2026**, *8*, 151. [CrossRef]
3. National Bureau of Statistics of China. *Announcement on Grain Output Data for 2024*; National Bureau of Statistics of China: Beijing, China, 2024. Available online: https://www.stats.gov.cn/sj/zxfb/202412/t20241213_1957744.html (accessed on 16 August 2026).
4. Guanyan Report Network. China Plant-Protection Drone Industry: In-Depth Research and Investment Trend Forecast Report (2024–2031) (Annual Operating Area in 2023: 2.13 Billion Mu-Times). 2024. Available online: https://www.chinabaogao.com/detail/706206.html (accessed on 16 August 2026).
5. Getahun, S.; Kefale, H.; Gelaye, Y. Application of precision agriculture technologies for sustainable crop production and environmental sustainability: A systematic review. *Sci. World J.* **2024**, *2024*, 2126734. [CrossRef]
6. Kamilaris, A.; Prenafeta-Boldú, F.X. Deep learning in agriculture: A survey. *Comput. Electron. Agric.* **2018**, *147*, 70–90. [CrossRef]
7. Wolfert, S.; Ge, L.; Verdouw, C.; Bogaardt, M.J. Big data in smart farming—A review. *Agric. Syst.* **2017**, *153*, 69–80. [CrossRef]
8. Halachmi, I.; Guarino, M.; Bewley, J.; Pastell, M. Smart animal agriculture: Application of real-time sensors to improve animal well-being and production. *Annu. Rev. Anim. Biosci.* **2019**, *7*, 403–425. [CrossRef]
9. Gaillard, C.; Brossard, L.; Dourmad, J.-Y. Improvement of feed and nutrient efficiency in pig production through precision feeding. *Anim. Feed Sci. Technol.* **2020**, *268*, 114611. [CrossRef]
10. Lopez, B.M.; Kang, H.S.; Kim, T.H.; Viterbo, V.S.; Kim, H.S.; Na, C.S.; Seo, K.S. Optimization of swine breeding programs using genomic selection with ZPLAN+. *Asian-Australas. J. Anim. Sci.* **2016**, *29*, 640–645. [CrossRef]
11. Alexandratos, N.; Bruinsma, J. *World Agriculture Towards 2030/2050: The 2012 Revision (ESA Working Paper No. 12-03)*; FAO: Rome, Italy, 2012. Available online: https://www.fao.org/4/ap106e/ap106e.pdf (accessed on 16 August 2026).
12. FAO. *Food Security (Policy Brief, June 2006, Issue 2)*; FAO Agriculture and Development Economics Division: Rome, Italy, 2006. Available online: https://www.fao.org/fileadmin/templates/faoitaly/documents/pdf/pdf_Food_Security_Cocept_Note.pdf (accessed on 16 August 2026).
13. General Office of the CPC Central Committee; General Office of the State Council. Digital Village Development Strategy Outline. 2019. Available online: https://www.gov.cn/zhengce/2019-05/16/content_5392269.htm (accessed on 16 August 2026). (In Chinese)
14. National Agro-Tech Extension and Service Center. National Plant-Protection Drone Holdings and Operating Area, 2024 (Figures Released by NATESC at the 38th China Plant Protection Information Exchange and Pesticide and Machinery Trade Fair, Hefei, November 2024: 251,000 Units and 2.67 Billion Mu-Times Treated, Both up About 25% Year on Year. Farmers' Daily, Reprinted by China Agricultural University News, 27 November 2024). Available online: https://news.cau.edu.cn/mtndnew/d26d46e9fcf946ad9174171b9bad178a.htm (accessed on 16 August 2026).
15. Pereira, R.D.; Badino, A.C.; Cruz, A.J.G. Framework based on artificial intelligence to increase industrial bioethanol production. *Energy Fuels* **2020**, *34*, 4670–4677. [CrossRef]
16. National Bureau of Statistics of China. Statistical Communiqué of the People's Republic of China on the 2024 National Economic and Social Development (Urbanization Rate of Permanent Residents: 67.0% at End-2024). 2025. Available online: https://www.stats.gov.cn/sj/zxfb/202502/t20250228_1958817.html (accessed on 16 August 2026).
17. Gustavsson, J.; Cederberg, C.; Sonesson, U.; van Otterdijk, R.; Meybeck, A. *Global Food Losses and Food Waste—Extent, Causes and Prevention*; FAO: Rome, Italy, 2011. Available online: https://www.fao.org/4/mb060e/mb060e.pdf (accessed on 16 August 2026).
18. Yao, M.; McCrory, M.A.; Ma, G.; Li, Y.; Dolnikowski, G.G.; Roberts, S.B. Energy requirements of urban Chinese adults with manual or sedentary occupations, determined using the doubly labeled water method. *Eur. J. Clin. Nutr.* **2002**, *56*, 575–584. [CrossRef]
19. Xinhua News Agency. Tianjin Port Automates Nearly 90% of Large-Scale Container Equipment 2025. Available online: https://jp.news.cn/20250622/f6f2dced93c7455f978bf6953f2e6b2e/c.html (accessed on 16 August 2026).
20. Guan, R.; Wu, J.; Wang, Y.; Cai, Q.; Li, X. Comparative analysis of productive performance and fattening efficiency of commercial pigs in China for two consecutive years. *Sci. Rep.* **2023**, *13*, 8154. [CrossRef]
21. Li, H.; Chen, J.; Li, X.; Gan, J.; Liu, H.; Jian, Z.; Xu, S.; Zhang, A.; Li, G.; Chen, K. Artificial neural network and genetic algorithm coupled fermentation kinetics to regulate L-lysine fermentation. *Bioresour. Technol.* **2024**, *393*, 130151. [CrossRef]
22. Yang, X.; Chen, N.; Yu, H.; Liu, X.; Feng, Y.; Xing, D.; Tian, Y. Applying machine learning and genetic algorithms accelerated for optimizing ethanol production. *Sci. Total Environ.* **2024**, *955*, 177027. [CrossRef]
23. Zheng, Q.; Ha, T.; Prishchepov, A.V.; Zeng, Y.; Yin, H.; Koh, L.P. The neglected role of abandoned cropland in supporting both food security and climate change mitigation. *Nat. Commun.* **2023**, *14*, 6083. [CrossRef] [PubMed]
24. Wu, X.; Zhao, N.; Wang, Y.; Ye, Y.; Wang, W.; Yue, T.; Zhang, L.; Liu, Y. The potential role of abandoned cropland for food security in China. *Resour. Conserv. Recycl.* **2025**, *212*, 108004. [CrossRef]

25. Cheng, P.; Wang, Y.; Liu, K.; Kong, X.; Tang, H.; Cheng, Y.; Chen, J. Why do farmers leave land idle? Unpacking the role of farmland fragmentation and mechanization constraints in farmland abandonment behavior. *Land* **2026**, *15*, 1315. [CrossRef]
26. Jiang, Y.; Jiang, Y.; Guo, X.; Guo, Z.; Ye, Y.; Huang, J.; Liu, J. Monitoring of farmland abandonment based on Google Earth Engine and interpretable machine learning. *Agriculture* **2025**, *15*, 2090. [CrossRef]
27. Cheng, P.; Zhang, Y.; Liu, K.; Kong, X.; Wu, S.; Yan, H.; Jiang, P. Continuing the continuous harvests of food production: From the perspective of the interrelationships among cultivated land quantity, quality, and grain yield. *Humanit. Soc. Sci. Commun.* **2025**, *12*, 46. [CrossRef]
28. Li, J.; Ma, W.; Shen, B.; Li, L. Can unmanned aerial vehicle (UAV) adoption reduce pesticide use and enhance yields? Evidence from mountainous rice farming in Yunnan, China. *Food Policy* **2025**, *136*, 102965. [CrossRef]
29. Wang, G.; Lan, Y.; Yuan, H.; Qi, H.; Chen, P.; Ouyang, F.; Han, Y. Comparison of spray deposition, control efficacy on wheat aphids and working efficiency in the wheat field of the unmanned aerial vehicle with boom sprayer and two conventional knapsack sprayers. *Appl. Sci.* **2019**, *9*, 218. [CrossRef]
30. FAO. *FAOSTAT: Food Balances (2010–) and Crops and Livestock Products [Data Set]*; Food and Agriculture Organization of the United Nations: Rome, Italy, 2025. Available online: https://www.fao.org/faostat/en/#data (accessed on 10 July 2026).
31. Sheng, Y.; Tian, X.; Qiao, W.; Peng, C. Measuring agricultural total factor productivity in China: Pattern and drivers over the period of 1978–2016. *Aust. J. Agric. Resour. Econ.* **2020**, *64*, 82–103. [CrossRef]
32. European Commission. Directorate-General for Agriculture and Rural Development. Approved 28 CAP Strategic Plans (2023–2027): Summary Overview for 27 Member States—Facts and Figures 2023. Available online: https://agriculture.ec.europa.eu/system/files/2023-06/approved-28-cap-strategic-plans-2023-27.pdf (accessed on 16 August 2026).
33. Council of the European Communities. Council Directive 91/676/EEC of 12 December 1991 concerning the protection of waters against pollution caused by nitrates from agricultural sources. *Off. J. Eur. Communities* **1991**, *L 375*, 1–8. Available online: https://eur-lex.europa.eu/legal-content/EN/TXT/?uri=CELEX:31991L0676 (accessed on 16 August 2026).
34. European Commission. *A Farm to Fork Strategy for a Fair, Healthy and Environmentally-Friendly Food System (COM(2020) 381 Final)*; European Commission: Brussels, Belgium, 2020. Available online: https://eur-lex.europa.eu/legal-content/EN/TXT/?uri=CELEX:52020DC0381 (accessed on 16 August 2026).
35. McFadden, J.; Njuki, E.; Griffin, T. *Precision Agriculture in the Digital Era: Recent Adoption on U.S. Farms (Economic Information Bulletin No. 248)*; U.S. Department of Agriculture, Economic Research Service: Washington, DC, USA, 2023. Available online: https://www.ers.usda.gov/publications/105893 (accessed on 16 August 2026).
36. Lowenberg-DeBoer, J.; Erickson, B. Setting the record straight on precision agriculture adoption. *Agron. J.* **2019**, *111*, 1552–1569. [CrossRef]
37. Ministry of Agriculture, Forestry and Fisheries of Japan. Annual Report on Food, Agriculture and Rural Areas in Japan, FY2024 (Core Agricultural Workers 1.114 Million in 2024, Mean Age 69.2; Abandoned Farmland 257,000 ha). 2025. Available online: https://www.maff.go.jp/j/wpaper/w_maff/r6/r6_h/index.html (accessed on 16 August 2026).
38. Ministry of Agriculture, Forestry and Fisheries of Japan. Annual Report on Food, Agriculture and Rural Areas in Japan, FY2024, Feature 3: Use and Outlook of Smart Agricultural Technology (Act on Promotion of Smart Agricultural Technology, Act No. 63 of 2024: Passed 14 June 2024, Promulgated 21 June 2024, in Force 1 October 2024). 2025. Available online: https://www.maff.go.jp/j/wpaper/w_maff/r6/r6_h/trend/part1/chap0/c0_1_03.html (accessed on 16 August 2026).

Disclaimer/Publisher's Note: The statements, opinions and data contained in all publications are solely those of the individual author(s) and contributor(s) and not of MDPI and/or the editor(s). MDPI and/or the editor(s) disclaim responsibility for any injury to people or property resulting from any ideas, methods, instructions or products referred to in the content.